

## Rotational Degrees of Freedom of Molecules in Solids. I. The Cyanide Ion in Alkali Halides

W. D. SEWARD\* AND V. NARAYANAMURTI†

*Laboratory of Atomic and Solid State Physics, Cornell University, Ithaca, New York*

(Received 28 January 1966)

By means of infrared-absorption, thermal-conductivity, and specific-heat measurements at low temperatures, the problem of rotational motion of molecules in solids has been studied using  $\text{CN}^-$  ions substituted for the halogen in KCl, KBr, KI, RbCl, NaCl, and NaBr. Energy levels associated with the ion performing free rotation, hindered rotation, oscillation, and tunneling motion were observed. It was found that a simple 3-dimensional potential for a linear diatomic molecule developed by Devonshire based on a 2-dimensional cosine potential first proposed by Pauling explained all of our observations. For the potassium halides the barrier height is 0.003 eV; in RbCl it is 0.0075 eV, and in the sodium halides it is  $>0.015$  eV. Stress experiments show that the ion has 6 equilibrium orientations along the (100) directions. Strong phonon scattering by tunneling states and rotational states is observed. The scattering can be quantitatively described with a Lorentzian resonance cross section.

### I. INTRODUCTION

A FREE molecule containing  $N$  atoms has  $3N-6$  degrees of vibrational freedom, 3 degrees of translational freedom, and 3 degrees of rotational freedom. When a molecule is introduced substitutionally into a lattice, the vibrational degrees of freedom are usually changed relatively little by the matrix. The translational degrees of freedom of the molecule are the same as the translational degrees of freedom of an impurity atom, i.e., they manifest themselves as impurity modes. In this work, we have considered the third group of degrees of freedom, those connected with the rotational inertia of the molecule.

The present study originated from the study of phonon-defect interactions through measurements of the low-temperature lattice thermal conductivity initiated in this laboratory by Sproull and co-workers. Klein<sup>1</sup> noticed that NaCl crystals grown in air had an extremely low thermal conductivity of a very peculiar temperature dependence. He was able to relate this phonon scattering to some molecular impurities which absorbed light of  $186\text{-m}\mu$  wavelength. This defect has since been identified by him as the  $\text{OH}^-$  ion.<sup>2</sup> In his thesis,<sup>3</sup> Klein speculated that the strong phonon scattering was associated with the rotational degrees of freedom of the impurity ion. A study of these defects and their interactions with the phonons was complicated by the fact that he could not detect the  $\text{OH}^-$  ions in NaCl by IR spectroscopy. In KCl, the infrared O-H stretching vibration was extremely weak.<sup>4</sup> The cause for this peculiar influence of the host lattice is still unknown.<sup>5</sup>

\* Present address: Department of Physics, University of Illinois, Urbana, Illinois.

† Present address: Department of Physics, Indian Institute of Technology, Bombay, India.

<sup>1</sup> M. V. Klein, Phys. Rev. **122**, 1393 (1961).

<sup>2</sup> M. V. Klein, Bull. Am. Phys. Soc. **10**, 348 (1965).

<sup>3</sup> M. V. Klein, Ph.D. thesis, Cornell University, 1960 (unpublished).

<sup>4</sup> M. V. Klein, Bull. Am. Phys. Soc. **8**, 230 (1963).

<sup>5</sup> The small dipole moment observed in the IR absorption is in striking contrast to the result obtained in dielectric measurements

In following up Klein's suggestions we have studied  $\text{CN}^-$  and  $\text{NO}_2^-$  in a number of alkali halide host lattices. These molecules show infrared absorptions of the theoretically expected strength. Hence, it appears that the trapping of the molecule ion in the lattice vacancy does not affect its vibrational properties very much. We wish to show how a combined use of photon and phonon spectroscopy (infrared absorption and thermal conductivity measurements) and of specific heat measurements can yield a detailed picture of the rotational degrees of freedom of molecular ions in solids and of their phonon scattering cross sections. This paper deals with the  $\text{CN}^-$  ion. We shall see that this is a particularly simple case. On the other hand, the more complicated  $\text{NO}_2^-$  ion gives a deeper insight into the variety of rotational and translational degrees of freedom which are possible for a molecule in a solid in the most general case. This will be discussed in the following paper.<sup>6</sup> Part of the work reported here has been briefly discussed previously.<sup>7-10</sup>

### II. EXPERIMENTAL TECHNIQUES

#### A. The IR Spectrophotometer

All infrared measurements between  $2.5\ \mu$  and  $15\ \mu$  were made with a Beckman IR-7 prism-grating spectrophotometer with NaCl optics. It is primarily designed for double beam operation at ambient tempera-

where a dipole moment  $\mu \sim 2$  D was found. See Bulletin of the International Conference on Color Centers, Urbana, 1965 (unpublished) for recent references.

<sup>6</sup> V. Narayanamurti, W. D. Seward, and R. O. Pohl, following paper, Phys. Rev. **148**, 481 (1966).

<sup>7</sup> R. O. Pohl, Phys. Rev. Letters **8**, 481 (1962); and Z. Physik **176**, 358 (1963).

<sup>8</sup> W. D. Seward, in *Proceedings of the Ninth International Conference on Low Temperature Physics, Columbus, Ohio, 1964*, edited by J. G. Daunt *et al.* (Plenum Press, Inc., New York, 1965), p. 1130.

<sup>9</sup> V. Narayanamurti, Phys. Rev. Letters **13**, 693 (1964).

<sup>10</sup> V. Narayanamurti, Bull. Am. Phys. Soc. **10**, 390 (1965); V. Narayanamurti and R. O. Pohl, *ibid.* **10**, 616 (1965); W. D. Seward, *ibid.* **10**, 617 (1965).

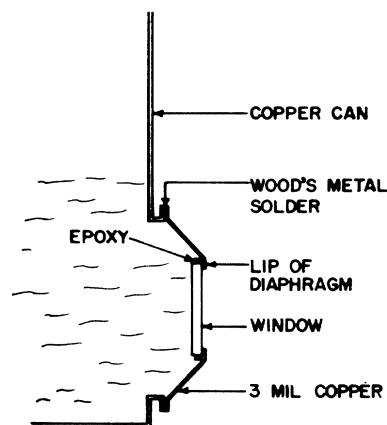


FIG. 1. Schematic of the window arrangement used in the immersion cryostat.

tures. In order to make measurements at low temperatures with small samples the spectrometer was modified<sup>11</sup> so that the beam having passed through the monochromator, was focussed onto the sample. The cross section of the beam striking the sample<sup>12</sup> was  $1\text{ cm} \times 0.01\text{ cm}$  (at  $2100\text{ cm}^{-1}$ ) instead of  $2.5\text{ cm} \times 0.6\text{ cm}$  when placed in the usual compartment of the IR-7. The use of monochromatic light also reduces the radiation heating of the sample and avoids a possible radiation-induced change in population of the energy states of the molecule. The resolution obtained at low temperatures was  $0.3\text{ cm}^{-1}$  between  $1000\text{ cm}^{-1}$  and  $1300\text{ cm}^{-1}$ , and  $0.6\text{ cm}^{-1}$  at  $2100\text{ cm}^{-1}$ . Measurements between  $2.0\text{ }\mu$  ( $5000\text{ cm}^{-1}$ ) and  $2.45\text{ }\mu$  ( $4000\text{ cm}^{-1}$ ) were made with a Cary Model-14 spectrophotometer. Its resolution was approximately  $5 \times 10^{-3}\text{ }\mu$  ( $1\text{ cm}^{-1}$ ).

### B. IR Cryogenics

Measurements above  $4.2^\circ\text{K}$  were made with conduction cryostats of conventional design. The use of LiF cold windows mounted on the liquid  $\text{N}_2$  radiation shield decreased the lowest temperature obtained from  $13$  to  $7^\circ\text{K}$ . Higher temperature measurements were made during the warmup. Temperature measurements were made with  $1000\text{-}\Omega$  and  $1500\text{-}\Omega$   $\frac{1}{10}\text{-W}$ , calibrated<sup>13</sup> Allen-Bradley carbon resistors.

Measurements below  $4.2^\circ\text{K}$  were made with an immersion cryostat. The difficulty here is to make a seal between an infrared transmitting window and the helium chamber which does not crack upon cooling and is tight to superfluid helium. A similar technique for an exchange gas cryostat has been described by Roberts.<sup>14</sup>

<sup>11</sup> We are grateful to Dr. D. Fröhlich for having borne a major load of the work involved in this modification. For details of the modified instrument see V. Narayanamurti, Ph.D. thesis, Cornell University, 1964 (unpublished).

<sup>12</sup> The cross section varies slightly with wavelength since the slit width is varied with wavelength.

<sup>13</sup> These resistors were calibrated against a gas thermometer in the Cornell thermal conductivity equipment by Dr. C. T. Walker, Dr. F. Baumann, and Dr. P. D. Thacher.

<sup>14</sup> V. Roberts, *J. Sci. Instr.* **31**, 251 (1954); **32**, 294 (1955).

An expanded view of the window arrangement is shown in Fig. 1. A 1-in.-diam circular  $\text{CaF}_2$  window was epoxyed to a well annealed 3-mil copper diaphragm with Hysol 4314 epoxy resin. The diaphragm was soldered with Wood's metal to the copper liquid-helium can. The most successful pair of windows has been cycled to  $\lambda$  helium temperatures more than 100 times and is still in use. The least successful pair was cycled only twice. For measurements out to  $13.5\text{ }\mu$ , Irtran-2 windows (obtained from Eastman Kodak Company, Rochester) were used. KCl and KBr windows were also tried but were unsuccessful. With and without "cold" LiF windows on the nitrogen radiation shield, the lowest temperatures attained in the cryostat were<sup>15</sup>  $1.36$  and  $1.55^\circ\text{K}$ , respectively. With the LiF "cold" windows the bubbling of the normal helium was sufficiently small to enable steady-state measurements to be made at  $4.2^\circ\text{K}$ . For measurements between the  $\lambda$  point and  $4.2^\circ\text{K}$ , the bath was first pumped to a temperature below the desired temperature. A pressure gradient was then set up along the length of the helium path by closing the valves to the helium pumping system. Once the desired temperature was reached, the temperature was maintained for long periods of time with very little bubbling of the He bath by pumping through a  $\frac{1}{8}$ -in. needle valve.

The immersion cryostat was also used for studying changes in the  $\text{CN}^-$  absorption spectrum under the influence of a static electric field or uniaxial stress. For electric fields parallel to the direction of the incident light nickel meshes (50 lines/in.) were used as electrodes.<sup>16</sup> An electric field perpendicular to the direction of the incident light was applied by means of metal electrodes.

For the uniaxial-stress measurements the crystals were mounted on a slotted cylinder to allow passage of the IR beam. The stress was applied perpendicular to the direction of the incident beam<sup>17</sup> with a hydraulic pump. In order to obtain uniform strain, J oil was applied to the crystal surfaces. Several stress runs were made and the data presented in Sec. IV represent an average of all the runs.

### C. Thermal Conductivity

The thermal conductivity was measured using the standard steady-state method in a  $\text{He}^4$  cryostat<sup>18,19</sup> and in a  $\text{He}^3$  cryostat that was built for measurements between  $0.3^\circ$  and  $2.0^\circ\text{K}$ .<sup>20</sup> Figure 2 is a cross section of the experimental chamber of the  $\text{He}^3$  cryostat showing

<sup>15</sup> The temperature of the bath was measured with a  $56\text{ }\Omega$  calibrated Allen-Bradley resistor. The temperature difference between the crystal and the bath is estimated to be less than  $0.01^\circ\text{K}$ .

<sup>16</sup> The meshes were obtained from Buckbee Mears Company, St. Paul, Minnesota.

<sup>17</sup> The grating of our spectrometer polarizes about 80% of the incident beam perpendicular to the axis of the uniaxial stress.

<sup>18</sup> G. A. Slack, *Phys. Rev.* **105**, 832 (1957).

<sup>19</sup> W. S. Williams, *Phys. Rev.* **119**, 1021 (1960).

<sup>20</sup> W. D. Seward, Ph.D. thesis, Cornell University, 1965 (unpublished).

TABLE I. Spectroscopic determination of  $\text{CN}^-$  concentration. The concentration  $N_{\text{CN}^-}$  (in  $\text{cm}^{-3}$ ) is related to the peak absorption coefficient  $\alpha_{\text{CN}^-}$  (in  $\text{cm}^{-1}$ ) by the relation  $N_{\text{CN}^-} = \sigma_{\text{CN}^-} \alpha_{\text{CN}^-}$ . The values of  $\sigma_{\text{CN}^-}$  are given in the table together with the frequency,  $\tilde{\nu}_{\text{CN}^-}$ , of the  $\text{CN}^-$  stretching fundamental for the different alkali halides at room temperature. The constant  $\sigma$  was determined for each host lattice from a chemical analysis performed at the Analytical Facility of the Cornell Materials Science Center. The chemical determinations are believed to be good to 10% for all the alkali halides excepting KI and RbCl, which are good to 30%.

Host lattice	$\tilde{\nu}_{\text{CN}^-}$ ( $\text{cm}^{-1}$ )	$\sigma_{\text{CN}^-}$ ( $\text{cm}^{-2}$ )	Host lattice	$\tilde{\nu}_{\text{CN}^-}$ ( $\text{cm}^{-1}$ )	$\sigma_{\text{CN}^-}$ ( $\text{cm}^{-2}$ )
KCl	2105	$3.6 \times 10^{19}$	NaCl	2104	$1.8 \times 10^{19}$
KBr	2097	$3.1 \times 10^{19}$	NaBr	2086	$1.55 \times 10^{19}$
KI	2067	$6.7 \times 10^{19}$	RbCl	2075	$5.2 \times 10^{19}$

the position of the sample. Thermal contact to the crystal was made with indium-faced phosphor bronze clamps. The thermal gradient along the crystal was measured with Speer  $\frac{1}{2}$ -W, 470- $\Omega$ , grade 1002 carbon resistors which were calibrated in each run.<sup>21</sup> The primary temperature standard was a Honeywell germanium resistance thermometer, which had been initially calibrated using  $\text{He}^3$  and  $\text{He}^4$  vapor-pressure thermometers and a paramagnetic salt thermometer. All resistance measurements were made with an ac Wheatstone bridge having a maximum sensitivity for a 5000- $\Omega$  resistor of 1 part in  $10^4$  while only dissipating  $10^{-10}$  W in the resistor.<sup>20</sup>

#### D. Specific Heat

The specific-heat sample (mass 4 to 31 g) was cemented to a  $0.3 \times 0.4 \times 1.0$  cm support of either graphite or KCl heavily doped with KCN which was clamped to the crystal holder of the  $\text{He}^3$  cryostat. The thermometer, a  $\frac{1}{16}$ -W, 10- $\Omega$  Allen-Bradley resistor and a 1000- $\Omega$  Nichrome wire (0.025 mm) heater were secured to the crystal with varnish. A support with very low thermal conduction was necessary so that heat put into the crystal would leak out sufficiently slowly to allow the change in temperature and hence the specific heat to be measured. The time constant for the sample to approach the bath temperature was always at least 20 times longer than the duration of the heat pulse and the response time of the thermometry. The validity of the technique was tested on pure KCl (see Fig. 21) whose specific heat was found to be proportional to  $T^3$  with a Debye  $\Theta$  of  $229 \pm 2^\circ\text{K}$  compared to  $233 \pm 3^\circ\text{K}$  as given by Keesom and Pearlman.<sup>22</sup>

### III. CRYSTALS

The crystals were pulled from the melt in the Crystal Growing Facility of the Materials Science Center at Cornell from halogen-treated analytic reagent-grade material to which the proper amount of dopant had

<sup>21</sup> After 10–15 runs the Speer resistors would become noisy below  $0.5^\circ\text{K}$  and had to be replaced by a fresh pair.

<sup>22</sup> P. H. Keesom and N. Pearlman, Phys. Rev. **91**, 1354 (1953).

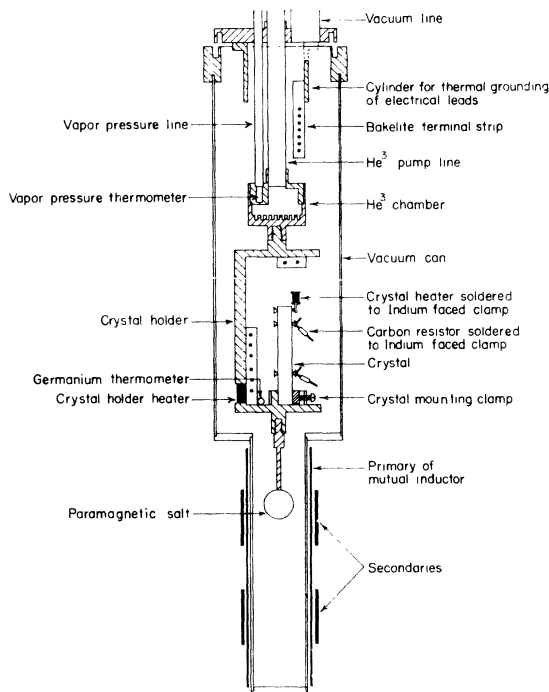


Fig. 2. Cross-sectional view of the experimental chamber of the  $\text{He}^3$  cryostat.

been added, using alumina, platinum or pyrolytic graphite crucibles and purified (through a Ti-Zr trap at  $350^\circ\text{C}$ ) argon as protective atmosphere. The crystals were about 10 cm long and 1.5 cm in diameter and clear except for the highest doping (0.5 mole % in the melt) which showed signs of precipitation at the bottom. These portions were discarded. For the spectroscopic determination of the  $\text{CN}^-$  concentrations, we refer to Table I.

In the infrared the only impurity within the limit of detectability (absorption coefficient  $\alpha < 10^{-2} \text{cm}^{-1}$ ) was  $\text{NCO}^-$ .<sup>23,24</sup> In the ultraviolet rudimentary "OH" bands were found. In the 0.5-mole %  $\text{CN}^-$ -doped crystals the absorption coefficient of this band was of the order of

<sup>23</sup> The frequencies of the observed infrared lines were in good agreement with those reported earlier by A. Maki and J. C. Decius, J. Chem. Phys. **28**, 1003 (1958), and by W. C. Price, W. F. Sherman, and G. R. Wilkinson, Proc. Roy. Soc. (London) **A255**, 5 (1960); Spectrochim. Acta **16**, 663 (1960). The maximum concentration of  $\text{NCO}^-$  in our 0.5 mole% KCN doped crystals was approximately  $5 \times 10^{18} \text{cm}^{-3}$ . This was determined by R. Pompei by melting a known concentration of  $\text{KCl} + \text{KNCO}$  between sapphire plates and then measuring the infrared absorption coefficient of the strong antisymmetric  $\nu_3$  fundamental at  $2182 \text{cm}^{-1}$  in KCl. From this  $\sigma_{\text{NCO}^-} = 7 \times 10^{17} \text{cm}^{-2}$  (see Table I) was determined.

<sup>24</sup> The characteristic absorption peaks of  $\text{NCO}^-$  are extremely sharp and have a half-width of about  $1.5 \text{cm}^{-1}$  at room temperatures in all host lattices studied. Closely spaced satellites approximately  $4 \text{cm}^{-1}$  away in KCl and KBr and  $2.5 \text{cm}^{-1}$  in KI are also observed and ascribed to librational motion. They were previously reported by Maki and Decius (Ref. 23). More recently Decius *et al.* explained these lines with interaction between adjacent  $\text{NCO}^-$  ions; J. C. Decius, J. L. Jacobson, W. F. Sherman, and G. R. Wilkinson, J. Chem. Phys. **43**, 2180 (1965).

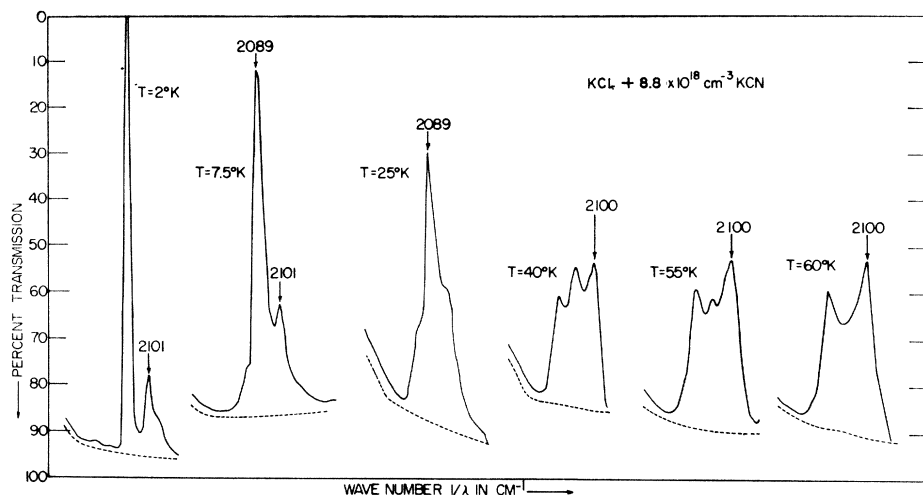


FIG. 3. Transmission spectra of 5-mm thick KCl crystal containing  $8.8 \times 10^{18} \text{ cm}^{-3}$   $\text{CN}^-$  ions. Fundamental vibration of  $\text{CN}^-$ .

$1 \text{ cm}^{-1}$  in all the alkali halides. In the "pure" samples this absorption was of the order of  $0.1 \text{ cm}^{-1}$  or less. The origin of the uv absorption band in cyanide-doped alkali halides has been ascribed to  $\text{NCO}^-$  by Akpınar<sup>25</sup> and to  $\text{OH}^-$  by Rolfe *et al.*<sup>26</sup> The thermal conductivity measurements<sup>27</sup> indicate that the ultraviolet absorption in our doped crystals is probably not due to  $\text{OH}^-$ .

From ionic conductivity measurements on KCl containing  $4 \times 10^{19} \text{ cm}^{-3}$   $\text{CN}^-$  between 200 and  $400^\circ\text{C}$  performed by J. Peech, it was concluded that the vacancy concentration was the same as in our undoped crystals, i.e., at most 5 ppm. This is as expected for the singly charged  $\text{CN}^-$  ion sitting in a substitutional site. On the other hand, doping with negative ions like  $\text{OH}^-$ ,  $\text{CO}_3^{2-}$ ,  $\text{SO}_4^{2-}$  has been found to significantly affect the ionic conductivity due to association either with positive divalent ions or vacancies.<sup>28-30</sup>

In summary it may be said that in our crystals the primary impurity other than  $\text{CN}^-$  is the  $\text{NCO}^-$ . Infrared (IR) and ionic-conductivity measurements indicate that the absorption in the cyanide stretching region is due to the singly charged  $\text{CN}^-$  ion in a substitutional site. Further confirmation of this picture together with details of the  $\text{CN}^-$  infrared absorption spectrum is presented in the next two sections.

The sizes of the samples used for the low-temperature IR measurements varied from 0.5 to 12 mm in thickness and usually had a cross section of  $1 \text{ cm}^2$ . The stress

samples were usually  $3.5 \times 3.5 \times 12 \text{ mm}$  with the long axis being the direction of uniaxial stress. The electric field samples were between 0.5 to 1 mm thick and  $1 \text{ cm}^2$  in cross section. The field was applied along the small dimension.

The thermal conductivity samples were  $5 \times 5 \times 40 \text{ mm}$  in size except samples for electric field measurements which were  $6 \times 2 \times 40 \text{ mm}$ . Electric fields were applied with evaporated gold electrodes 500–1000 Å thick. The surfaces of the cleaved crystals were sand-blasted in order to ensure diffuse phonon scattering by the boundaries.

## IV. INFRARED ABSORPTION RESULTS

### A. Absorption Spectra

In Figs. 3 and 4 we compare the spectrum of the fundamental and the overtone vibration of  $\text{CN}^-$  in KCl. Their features are almost identical. At  $2^\circ\text{K}$  the spectrum consists of a central line at  $2089 \pm 1 \text{ cm}^{-1}$  ( $4151 \text{ cm}^{-1}$  for the overtone) with a weak sum satellite  $12 \pm 1 \text{ cm}^{-1}$  away.<sup>31</sup> At about  $8^\circ\text{K}$  a weak difference satellite arises. It is less well resolved, and its separation is  $8 \pm 2 \text{ cm}^{-1}$  ( $9 \pm 2 \text{ cm}^{-1}$  for the overtone). At  $T = 25^\circ\text{K}$  the central peak's intensity decreases while the sum and difference satellites increase in intensity and the satellites shift in position toward the central peak. As the temperature increases to  $40^\circ\text{K}$ , the central peak further diminishes in intensity, but two broad bands arise whose separation increases with increasing temperature. The separation of the broad bands is  $23 \pm 1.5 \text{ cm}^{-1}$  at  $80^\circ\text{K}$  and  $40 \pm 2.5 \text{ cm}^{-1}$  at  $295^\circ\text{K}$  for both spectra. At all temperatures the width of the observed absorptions is not limited by the instrumental resolution.

Figures 5 and 6 show the spectrum of the  $\text{CN}^-$  in

<sup>25</sup> S. Akpınar, *Ann. Physik* **37**, 429 (1940).

<sup>26</sup> J. Rolfe, F. R. Lipsett, and W. J. King, *Phys. Rev.* **123**, 447 (1961).

<sup>27</sup> Our thermal-conductivity results for  $\text{NaCl} + \text{NaCN}$ , to be discussed later, show no low-temperature scattering whatsoever. Klein (Ref. 1) however, found a strong phonon scattering for NaCl doped with NaOH. The absorption coefficient was  $\sim 1 \text{ cm}^{-1}$  at  $190 \text{ m}\mu$  for our thermal-conductivity crystal.

<sup>28</sup> P. M. Gruzinsky and A. B. Scott, *J. Phys. Chem. Solids* **21**, 128 (1963).

<sup>29</sup> J. Rolfe, *Bull. Am. Phys. Soc.* **9**, 227 (1964); *Can. J. Phys.* **42**, 2195 (1964).

<sup>30</sup> B. Fritz, F. Lüty, and J. Anger, *Z. Physik* **174**, 240 (1963).

<sup>31</sup> The results reported here give a slightly more accurate re-determination of frequencies and concentrations reported in Ref. 9.

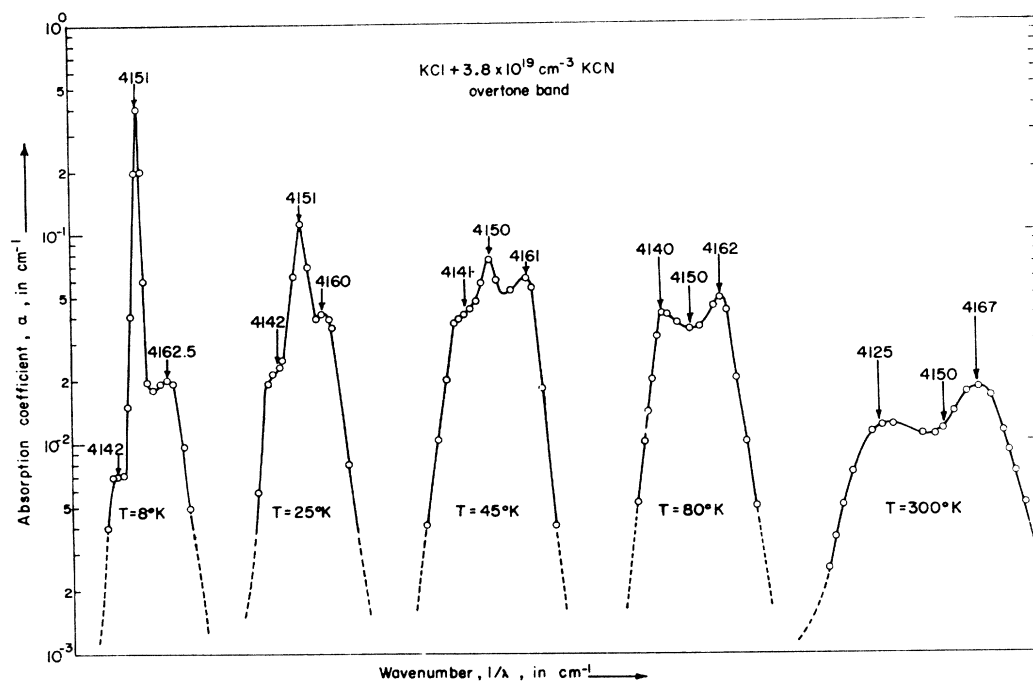


FIG. 4. Absorption spectra of the  $\text{CN}^-$  overtone vibration in KCl.

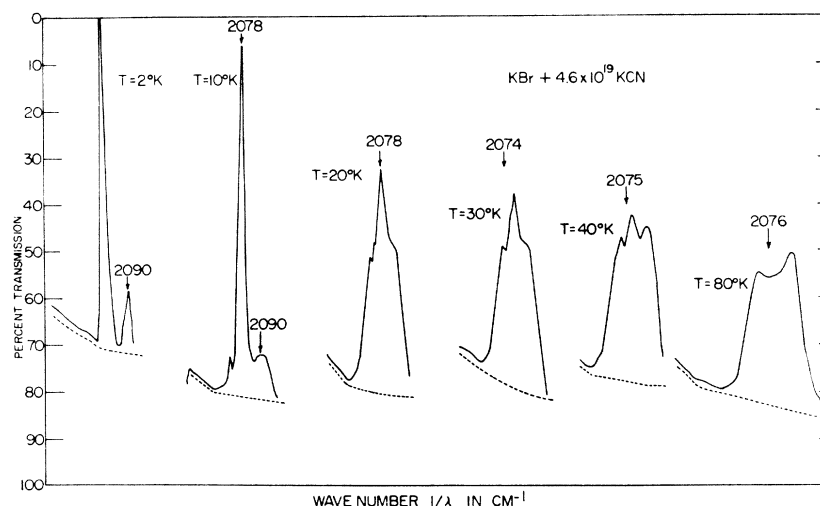


FIG. 5. Transmission spectra of 1.6-mm-thick KBr crystal containing  $4.6 \times 10^{19} \text{ cm}^{-3}$   $\text{CN}^-$  ions. Fundamental vibration of  $\text{CN}^-$ .

KBr for the fundamental and overtone vibrations.<sup>32</sup> Here again the separation of the sum satellite from the central line is about  $12 \text{ cm}^{-1}$ . The only differences between the KBr and KCl spectrum are that at high temperatures the central minimum is not so deep and that the separation between the broad bands at higher temperatures is slightly smaller,  $20 \pm 1.5 \text{ cm}^{-1}$  at  $80^\circ\text{K}$  and  $35 \pm 5 \text{ cm}^{-1}$  at  $295^\circ\text{K}$ .

<sup>32</sup> A weak sharp line at  $2074 \text{ cm}^{-1}$  which is probably due to  $\text{NCO}^-$  has been subtracted from the spectrum in Fig. 5. This line is definitely not due to  $\text{CN}^-$  since it was not observed in the overtone spectrum. [See also A. Maki and J. C. Decius, Ref. 23.]

The striking identity of the structure observed with fundamental and overtone vibrations proves that this structure is not merely the result of having the vibrational energy of some of the  $\text{CN}^-$  ions different from the majority because of different surroundings (clusters, interstitials etc.). If this were the case, the structure of the overtone absorption would have twice the width of the fundamental. Rather the structure is caused by a simultaneous excitation of the stretching vibration (with  $\Delta v=1$  for the fundamental and  $\Delta v=2$  for the overtone) plus or minus some other transitions, interpreted as librational or rotational ones in Ref. 9.

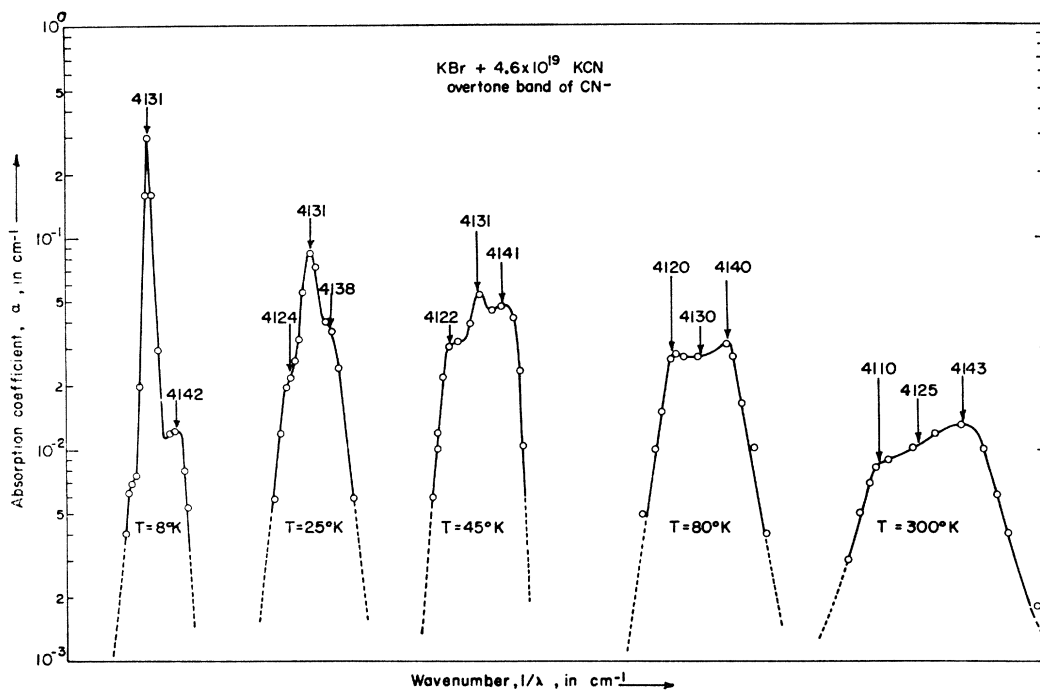


FIG. 6. Absorption spectra of  $\text{KBr} + 4.6 \times 10^{19} \text{ cm}^{-3} \text{ KCN}$ . Overtone vibration of  $\text{CN}^-$ .

Figure 7 shows the  $\text{CN}^-$  spectrum in KI at  $1.36^\circ\text{K}$ . Figure 8 shows the spectrum for higher temperatures. At  $T = 1.36^\circ\text{K}$  one again observes a central line with a weaker sum satellite about  $11 \text{ cm}^{-1}$  away and a barely resolvable difference satellite approximately  $2.5 \text{ cm}^{-1}$  away (at  $2064.5 \text{ cm}^{-1}$ ). In addition, broad bands are observed with maxima at approximately 2110, 2135, and  $2150 \text{ cm}^{-1}$ , i.e.,  $43 \text{ cm}^{-1}$ ,  $68 \text{ cm}^{-1}$ , and  $83 \text{ cm}^{-1}$  from the main  $\text{CN}^-$  line at  $2067 \text{ cm}^{-1}$ . At higher tempera-

tures the spectrum is very similar to that observed in KCl and KBr except that now the central minimum is no longer detectable. The half-width of the observed

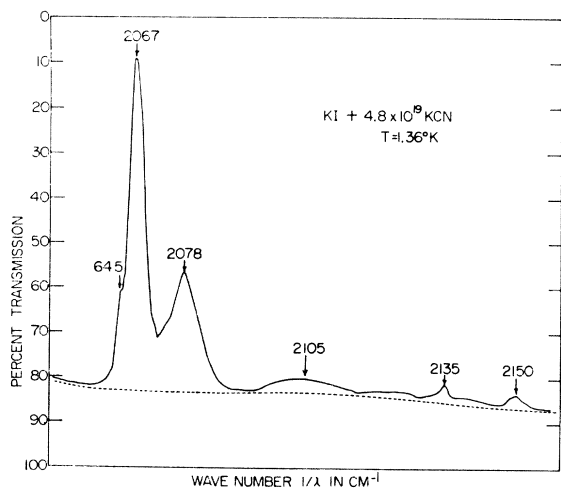


FIG. 7. Transmission spectra of 3 mm KI crystal containing  $\text{CN}^-$  ions at  $1.36^\circ\text{K}$ . Fundamental vibration. Notice the barely resolved shoulder at  $2064.5 \text{ cm}^{-1}$ . The wave-number scale is not the same as that for Figs. 3 and 5.

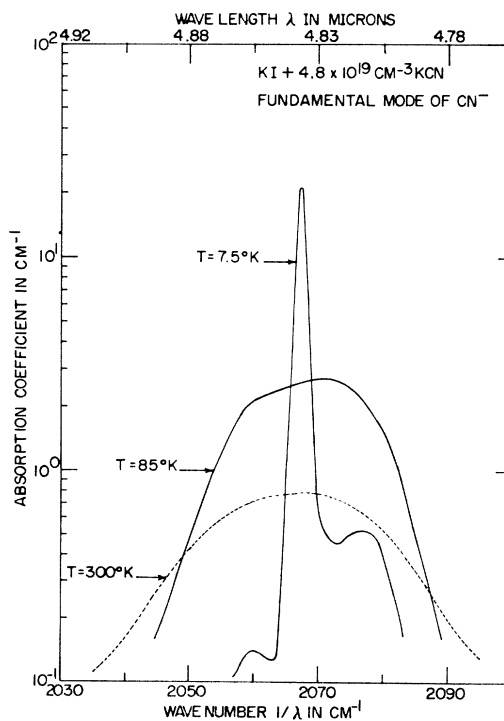


FIG. 8. Absorption spectra of  $\text{KI} + 4.8 \times 10^{19} \text{ cm}^{-3} \text{ KCN}$ . Fundamental vibration of  $\text{CN}^-$ .

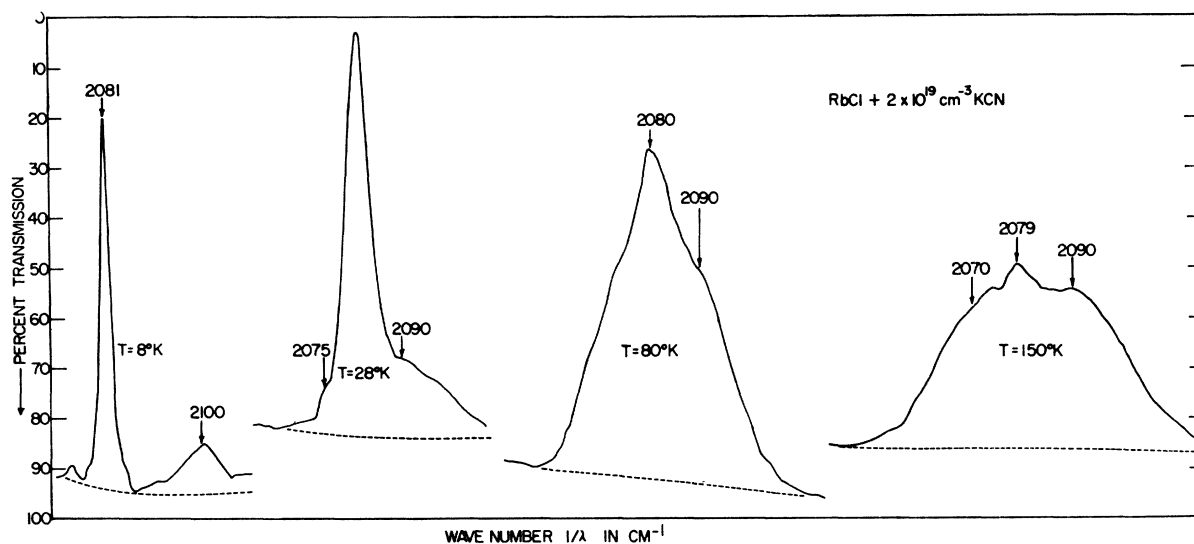


FIG. 9. Transmission spectra of 3.5 mm RbCl crystal containing  $2 \times 10^{19} \text{ cm}^{-3} \text{ CN}^-$  ions. Fundamental vibration.

broad band is  $22 \pm 1 \text{ cm}^{-1}$  at  $80^\circ\text{K}$  and  $40 \pm 2 \text{ cm}^{-1}$  at  $295^\circ\text{K}$ .

The  $\text{CN}^-$  spectrum in RbCl is qualitatively similar to that in the potassium salts, but the splitting of the sum satellite is now larger,  $19 \text{ cm}^{-1}$ , and the central line disappears only at about  $150^\circ\text{K}$ , see Fig. 9.

In NaCl and NaBr the spectrum consists of only one narrow band whose half-width is proportional to the square of the temperature, see Figs. 10 and 11. The instrumental resolution did not allow the determination of the line shape below  $80^\circ\text{K}$ .<sup>33</sup>

### B. Electric-Field and Stress Effects

The effect of a static electric field on the  $\text{CN}^-$  IR absorption in KCl:CN and NaCl:CN was studied at

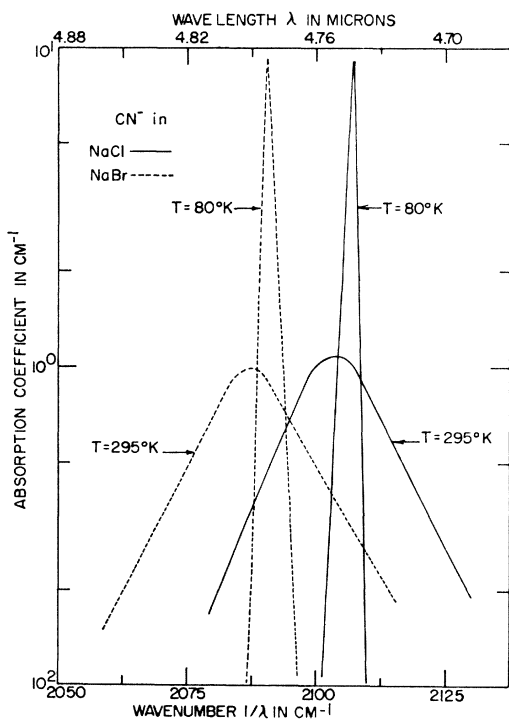


FIG. 10. Absorption spectra of  $\text{CN}^-$  fundamental vibration. Solid lines  $\text{NaCl} + 2 \times 10^{19} \text{ cm}^{-3} \text{ NaCN}$ , dashed lines  $\text{NaBr} + 1.6 \times 10^{19} \text{ cm}^{-3} \text{ NaCN}$ . The shift of the position of the peak absorption to higher energies at low temperatures is caused by the thermal contraction of the lattice.

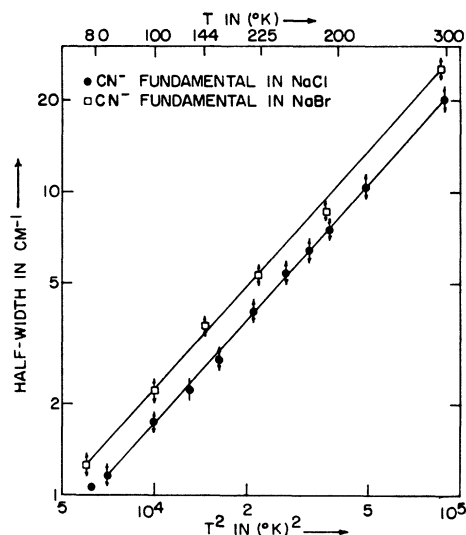


FIG. 11. Half-width of  $\text{CN}^-$  fundamental vibration as a function of temperature. Upper line:  $\text{NaBr} + 1.6 \times 10^{19} \text{ cm}^{-3} \text{ NaCN}$ , lower line:  $\text{NaCl} + 2 \times 10^{19} \text{ cm}^{-3} \text{ NaCN}$ .

<sup>33</sup> A weak *low-energy* satellite  $4 \text{ cm}^{-1}$  away from the main line was observed in NaCl (and NaBr) at low temperatures. With the overtone vibration a low-energy satellite  $8 \text{ cm}^{-1}$  away was observed. This suggests that these lines are to be associated with a different center, possibly  $\text{CN}^-$  in a different position in the lattice.

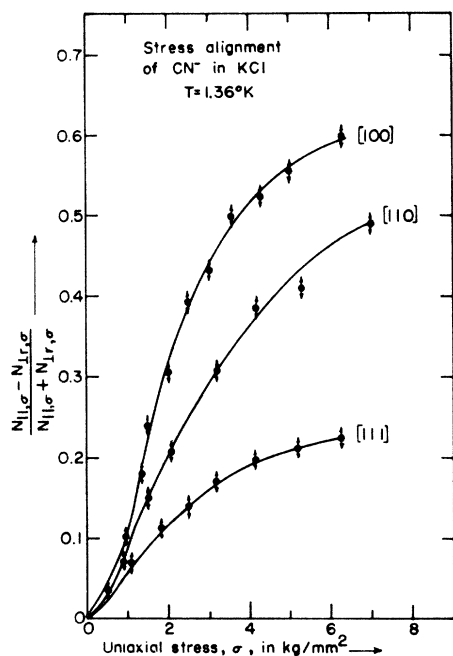


FIG. 12. Alignment of the  $\text{CN}^-$  ions as a function of uniaxial stress. KCl host lattice.  $T = 1.36^\circ\text{K}$ . For  $[110]$  stress the light was propagating in  $[110]$  direction (see also Ref. 57). The polarization showed no hysteresis upon removal of the stress. The polarization of the librational sum satellite was similar to that of the main band, although the accuracy was much poorer because of the smaller optical density.

$2^\circ\text{K}$ . The field was applied in  $[100]$  and  $[110]$  directions and was oriented both in the direction and perpendicular to the direction of the incident polarized light beam. For a maximum field of  $80 \text{ kV/cm}$ , the observed change in optical density was less than  $5\%$ . Under the assumption that the  $\text{CN}^-$  dumbbell carries a permanent moment  $\mu$  like a classical electric dipole, we conclude that the molecule is either frozen-in at  $2^\circ\text{K}$  or that  $\mu$  is small ( $< 0.3 \text{ D}$  if we use a Langevin-Debye expression for the polarization.) A distinction between these two possible explanations was achieved through uniaxial stress experiments. The observed change in optical density of the IR band<sup>34</sup> gives a direct measure of the number of molecules oriented parallel to the stress axis, denoted by  $N_{||,\sigma}$  and the number oriented perpendicular to the stress, denoted by  $N_{\perp,\sigma}$ . Stress alignment was found in KCl, KBr, KI, and RbCl. Figure 12 shows the directional dependence of the alignment at  $1.36^\circ\text{K}$  as a function of stress for KCl.

Figure 13 shows the temperature dependence<sup>35</sup> of the alignment between  $1.36$  and  $4.2^\circ\text{K}$ . It can be seen that for moderate stresses the alignment follows a  $1/T$  law.

<sup>34</sup> The transition dipole moment for the infrared stretching vibration of a diatomic molecule lies always along the internuclear axis.

<sup>35</sup> With very high stresses a slight narrowing of the absorption line was noticed. We also studied one crystal of  $\text{KCl}+\text{KCN}$  at  $77^\circ\text{K}$  and a stress of  $1 \text{ kg/mm}^2$ . No effect was detected.

The alignment observed in other host lattices is smaller. Figure 14 shows the results for  $[100]$  stresses in KCl, KBr, KI, and NaCl. As can be seen from the figure no alignment is observed<sup>36</sup> in NaCl and NaBr. After applying the uniaxial stress we waited 10 to 15 min and failed to detect any alignment in these two host lattices.<sup>37</sup> In all the other host lattices the alignment followed the stress within the time constant of our instrument (2 sec).

## V. THEORY AND DISCUSSION OF IR RESULTS

### A. Theory

Molecules in crystalline environments are expected to have discrete equilibrium orientations. Most of the features observed with  $\text{CN}^-$  in alkali halides can be explained with a simple two-well cosine potential, as shall be shown in the following. Thereafter we shall discuss how a quantitative description can be obtained by using a more realistic three-dimensional potential of octahedral symmetry.

Following Pauling<sup>38</sup> we choose a potential of the form

$$V = (V_0/2)(1 - \cos 2\theta). \quad (1)$$

The Schrödinger equation for this potential is known as Mathieu's equation and can be solved exactly.<sup>39</sup>

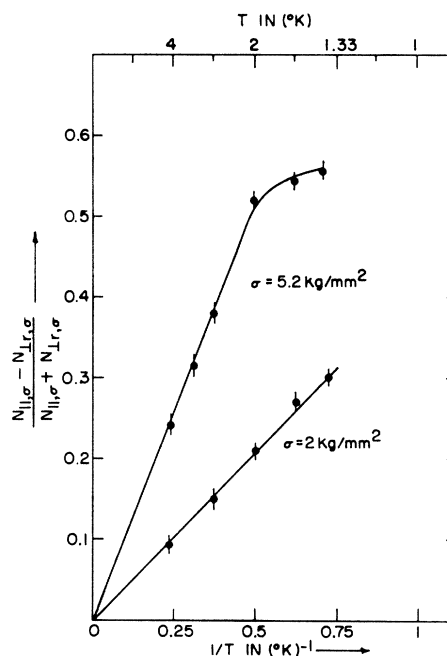


FIG. 13. Temperature dependence of the  $\text{CN}^-$  alignment in KCl for  $[100]$  uniaxial stress. Upper curve:  $\sigma = 5.2 \text{ kg/mm}^2$ . Lower curve:  $\sigma = 2 \text{ kg/mm}^2$ .

<sup>36</sup> This was studied between  $1.36$  and  $4.2^\circ\text{K}$  and for the  $[100]$   $[110]$  stress directions.

<sup>37</sup> The same results were obtained for  $\text{NCO}^-$  in KCl, KBr, and KI.

<sup>38</sup> L. Pauling, Phys. Rev. **36**, 430 (1930).

<sup>39</sup> *Tables Relating to Mathieu Functions* (Columbia University Press, New York, 1951).



When  $kT \ll V_0$ , the molecules occupy energy states below the top of the barrier. In the harmonic approximation these energy levels correspond to those of a harmonic oscillator

$$hc\tilde{\nu}_n^{\text{lib}} = hc\tilde{\nu}_0^{\text{lib}}(n + \frac{1}{2}), \quad (2)$$

with

$$\tilde{\nu}_0^{\text{lib}} = 2(\tilde{V}_0\tilde{B})^{1/2}. \quad (3)$$

Here  $\tilde{\nu}_0^{\text{lib}}$  is the fundamental librational frequency in  $\text{cm}^{-1}$  and  $\tilde{B} = h/8\pi^2cI$  is the rotational constant in  $\text{cm}^{-1}$  [All quantities<sup>40</sup> marked with a tilde ( $\sim$ ) are in  $\text{cm}^{-1}$ ]. Each energy level of the harmonic liblator is twofold degenerate for  $\tilde{\nu}_0^{\text{lib}} \ll \tilde{V}_0$ . In reality these levels are split due to the possibility of quantum-mechanical tunneling through the barrier which will be discussed later.

The selection rules for the degenerate liblator have been worked out by Hexter and Dows.<sup>41</sup> They showed that in the near-infrared vibrational spectrum the strongest transitions involve no changes in the librational quantum number, i.e., they give rise to the transition  $\Delta n = 0$  which is called the  $Q$  branch. Because of anharmonicity, weaker transitions  $\Delta n = \pm 1, \pm 2, \dots$ , etc. are allowed. These give rise to a succession of

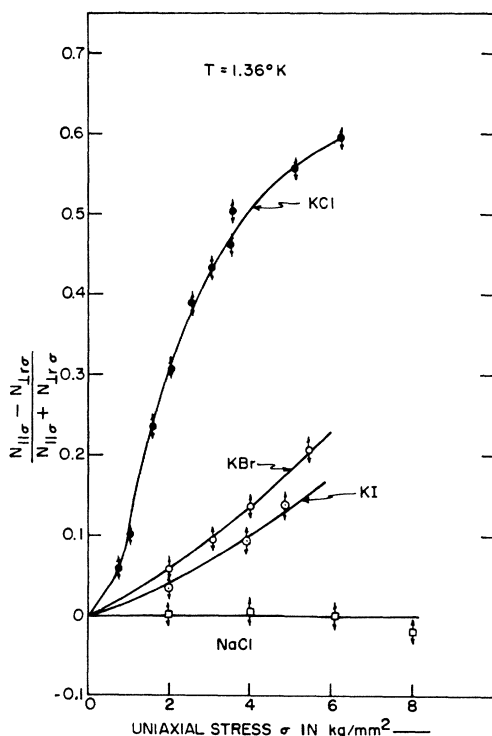


FIG. 14. Alignment of  $\text{CN}^-$  in different host lattices with  $[100]$  uniaxial stresses at  $T = 1.36^\circ\text{K}$ . The data for  $\text{RbCl}$  and  $\text{NaBr}$  (not shown in the figure) follow closely the curves for  $\text{KBr}$  and  $\text{NaCl}$ , respectively.

<sup>40</sup>  $1 \text{ cm}^{-1}$  corresponds to  $E = 1.24 \times 10^{-4} \text{ eV}$ ;  $f = 3 \times 10^{10} \text{ sec}^{-1}$ ;  $T = 1.42^\circ\text{K}$ .

<sup>41</sup> R. M. Hexter and D. A. Dows, *J. Chem. Phys.* **25**, 504 (1956).

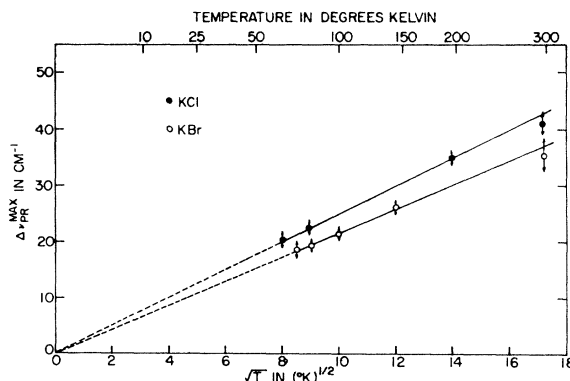


FIG. 15. Separation of the  $P$  and  $R$  maxima in  $\text{cm}^{-1}$  as a function of temperature. Upper line:  $\text{KCl} + 8.8 \times 10^{18} \text{ cm}^{-3} \text{ KCN}$ ; lower line  $\text{KBr} + 4.6 \times 10^{19} \text{ cm}^{-3} \text{ KCN}$ .

equally spaced lines which decrease in intensity by the factor

$$(\tilde{\nu}_0^{\text{lib}}/2\tilde{B})^{-\Delta n}.$$

In addition, the difference transitions are weaker than the sum transitions by the Boltzmann factor (thermal population).

The eigenstates with energies large compared to  $\tilde{V}_0$  correspond closely to those known for free molecules.<sup>42</sup> The free rotor energy levels are given by<sup>43</sup>

$$\tilde{\nu}_J^{\text{Rot}} = \tilde{B}J(J+1), \quad (4)$$

where  $J$  is the rotational quantum number. Each level is  $(2J+1)$ -fold degenerate. The selection rules for the vibrating rotator are  $\Delta J = \pm 1$ . The transitions with  $\Delta J = +1$  and  $\Delta J = -1$  give rise to the  $R$  and  $P$  branches, respectively, while the transitions with  $\Delta J = 0$  (the  $Q$  branch) are now forbidden.<sup>44</sup>

The shape of the vibration-rotation band is determined largely by the thermal population of the rotational levels. If one assumes that the intensity of the transitions from a given rotational state  $J$  is governed solely by the number of molecules in the state  $J$ , then the separation of the maxima in the  $P$  and  $R$  branches is given by<sup>45</sup>

$$\Delta\tilde{\nu}_{PR}^{\text{Max}} = (8\tilde{B}kT/hc)^{1/2} \propto T^{1/2}. \quad (5)$$

The results of the above simple theory may be briefly summarized as follows: at low temperatures ( $kT \ll V_0$ ) the infrared spectrum should consist of a strong  $Q$  branch with weak satellites separated from the fundamental by multiples of the librational frequency,

<sup>42</sup> We use the term "free rotation" for the case in which most of the molecules occupy energy states lying above the barrier.

<sup>43</sup> G. Herzberg, *Molecular Spectra and Molecular Structure* (D. Van Nostrand Company, New York, 1950), 2nd ed., Vol. I.

<sup>44</sup> The  $Q$  branch is forbidden only in the case of diatomic molecules. This makes it particularly easy to detect the transition from libration to rotation for such molecules. For more complicated molecules the  $Q$  branches are generally allowed thereby making the interpretation more difficult.

<sup>45</sup> Reference 43, p. 127.

$\bar{\nu}_0^{\text{lib}}$ . At high temperatures ( $kT \gg V_0$ ) the spectrum should approximate that known for free molecules, i.e., it should consist of *P* and *R* branches with a missing central *Q* branch. For intermediate temperatures ( $kT \approx V_0$ ) the spectrum should consist of *P*, *Q*, and *R* branches of comparable intensity.

Let us supplement this quantum-mechanical discussion of the states of rotational motion with the semiclassical picture of a rotating molecule: One can describe the states below the barrier  $V_0$  as oscillatory motions of the molecule in a particular well. This does not imply, however, that in these states the molecule cannot move from one well to the other. These states are therefore frequently called states of hindered rotation or states of almost free rotation. Such a change of the orientation is of particular interest if the influence of an electric or a stress field is studied. We can then describe the reorientation as a thermally activated rate process, involving a classical jumping of the molecule over the potential barrier with a "jump rate"  $\nu_{\text{jump}}$ :

$$\nu_{\text{jump}} = \nu_0^{\text{lib}} \exp\left(-\left(V_0 - \frac{1}{2}h\nu_0^{\text{lib}}/kT\right)\right). \quad (6)$$

It must be borne in mind that this description fails if the reorientation takes place through a tunnel process which is purely quantum mechanical.

### B. Comparison with Experiment

A qualitative comparison of the KCl and KBr data with the selection rules stated above indicates that at low temperatures (below about 20°K) the motion of the molecule can best be described as librational. Between 20 and 50°K the molecule performs hindered rotational motions, i.e., in this temperature region a significant number of molecules occupy energy states both above and below the barrier. Above 60°K most of the molecules occupy energy states lying above the barrier and now the characteristic *P* and *R* maxima of free molecules are observed. Figure 15 shows that the separation of the *P* and *R* maxima follows a  $T^{1/2}$  law as predicted by Eq. (5). From these data the rotational constant  $\bar{B} = 1.25 \text{ cm}^{-1}$  is obtained for the KCl host lattice. The error in determining  $\bar{B}$  by this method is determined by the width of the *P* and *R* maxima and is estimated to be about 20%. From  $\bar{B}$  the moment of inertia *I* and hence the internuclear separation between the C and N atoms is calculated to  $r = 1.4 \text{ \AA}$ .<sup>46</sup> Pauling<sup>47</sup> has estimated the radii of the carbon and nitrogen atoms to be 0.7 and 0.77 Å. From this a maximum value of 1.47 for the C-N bond length may be deduced. Recently

Elliott and Hastings<sup>48</sup> have used 1.16 Å for the C-N bond length in pure KCN in order to fit their neutron-diffraction data. Considering the simplicity of the model used here the agreement between calculation and experiment is considered very satisfactory.

From the above it follows that the motion of the  $\text{CN}^-$  in KCl and KBr is very nearly free at 60°K and above. Therefore the barrier height must be less than  $40 \text{ cm}^{-1}$ , (see Ref. 40). From Pauling's model the barrier height can also be determined directly from the librational frequency, using Eq. (3). One obtains  $\bar{V}_0 \approx 24 \text{ cm}^{-1}$ . The zero-point energy of the librator is  $6 \text{ cm}^{-1}$ , and hence the first librational state lies just below the barrier. The energy states above the barrier should approximate the free rotor levels closely. The rotational fine structure (separation =  $2\bar{B} \approx 2.5 \text{ cm}^{-1}$ ) has not been observed. The reason that only their envelope as *P* and *R* maxima is observed will be discussed later.

The above interpretation of the  $\text{CN}^-$  fundamental spectra in KCl and KBr is completely confirmed by the data for the  $\text{CN}^-$  overtone vibration in these host lattices. The overtone vibration shows a  $12 \text{ cm}^{-1}$  librational satellite at low temperatures and characteristic *P* and *R* maxima at high temperatures whose separation is the same, within experimental error, as that observed for the fundamental. The identity of the spectra for the fundamental and overtone vibrations indicates (1) that the interaction between vibration and rotation is negligible for the  $\text{CN}^-$  molecule and (2) that the barrier hindering rotation is independent of the vibrational state i.e., vibrational polarization effects are unimportant in determining the barrier hindering rotation.<sup>49</sup>

In RbCl the librational satellite is  $19 \text{ cm}^{-1}$  away so that  $\bar{V}_0$  for the twofold potential is about  $60 \text{ cm}^{-1}$ , i.e., the barrier height is about  $2\frac{1}{2}$  times that in KCl or KBr. This is confirmed by the temperature dependence of the spectra in RbCl which show *P* and *R* maxima only at very high temperatures ( $> 150^\circ\text{K}$ ) with a very weakly active *Q* branch.

The spectrum of  $\text{CN}^-$  in KI is similar to that observed in KCl and KBr at low temperatures. At high temperatures, however, the *P* and *R* branches are not resolved. Instead one obtains a broad absorption band of a width proportional to  $T^{1/2}$  (Fig. 16). These data closely resemble the data for the separation of the *P* and *R* maxima in KCl shown in Fig. 15. One might have expected a clear resolution of the *P* and *R* maxima in KI because the  $\text{I}^-$  cavity is large and hence the barrier

<sup>48</sup> N. Elliott and J. Hastings, *Acta Cryst.* **14**, 1018 (1961). Their results are, however, a matter of some controversy. See A. Sequeira, *Acta Cryst.* **18**, 291 (1965).

<sup>49</sup> This conclusion is evident also from the fact that the *Q*-branch frequencies change from host lattice to host lattice without bearing any obvious relation to the potential barrier hindering rotation. The barrier appears to be insensitive to the halide ion but very strongly dependent on the nearest-neighbor alkali ion. The reasons for this are unknown but experimentally the stress effects show that the  $\text{CN}^-$  dipole prefers to point towards the nearest-neighbor alkali ion.

<sup>46</sup> This is for KCl. For KBr one gets a smaller value of  $\bar{B}$  ( $1.0 \text{ cm}^{-1}$ ). The *P* and *R* branches are not as clearly resolved in KBr as in KCl which is probably due to center-of-mass motion of the molecule. See the discussion of the KI data in the text. The value of  $1.25 \text{ cm}^{-1}$  found in KCl will be assumed to be the true  $\bar{B}$  value for all host lattices.

<sup>47</sup> L. Pauling, *Nature of the Chemical Bond* (Cornell University Press, Ithaca, New York, 1948), 2nd ed., p. 164.

to rotation should be low. Yet there appears to be some mechanism disturbing the free rotation at high temperatures and causing the  $Q$  branch to become allowed. The selection rules for the librating molecule prefer the  $Q$  branch.<sup>41</sup> Similarly we suspect that for a molecule performing translational oscillations the  $Q$  branch may become allowed. Evidence for such a motion is given by the high-energy satellites observed at low temperatures, spaced 40, 68, and 83  $\text{cm}^{-1}$  from the main band. They may be caused by either of the following two mechanisms: (1) The 40- $\text{cm}^{-1}$  satellite may be associated with a resonant mode and the other two, narrower bands may be caused by excitations of local modes in the gap. Since the  $\text{CN}^-$  ion possesses symmetry  $C_{\infty v}$ , two translational local modes of symmetry  $A_1$  and  $E_1$  should be allowed, the  $A_1$  mode corresponding to translations along the internuclear axis and the doubly degenerate  $E_1$  mode corresponding to translations along axes perpendicular to the internuclear axis. In recent far-IR absorption measurements Lytle and Sievers<sup>50</sup> observed a strong absorption in  $\text{KI}:\text{CN}$  at 81.5  $\text{cm}^{-1}$  which they explained as a local mode in the gap, and broad absorptions between 35 and 70  $\text{cm}^{-1}$ , interpreted as resonant modes in the acoustic continuum. The spectrum was similar to that obtained in  $\text{KI}:\text{Cl}$ .<sup>51</sup> The absence of a second gap mode might be explained through rapid reorientational motion<sup>52</sup> of the  $\text{CN}^-$  ion about its two axes of inertia which causes it to behave like an ion of spherical symmetry. This model leaves the 68  $\text{cm}^{-1}$  mode observed in this work unexplained. (2) The center of mass of the ion may not coincide with the center of the large highly polarizable  $\text{I}^-$  cavity, as recently suggested by Pohl.<sup>53,54</sup> The close spacing of the difference satellite indicates that the potential to which the molecule is subjected in  $\text{KI}$  is different from that in  $\text{KCl}$ . Translational or librational motion around this off-center position may be responsible for some of the high-energy satellites.

The only conclusion that can be drawn at this stage is that the existence of some oscillatory motion (besides the one causing the 11  $\text{cm}^{-1}$  satellite) seems quite possible in the  $\text{KI}$  lattice and this may explain the persistence of the  $Q$  branch at high temperatures. The beginning of this may already be observed in  $\text{KBr}$  and  $\text{RbCl}$ .

The  $\text{CN}^-$  spectrum in  $\text{NaCl}$  and  $\text{NaBr}$  is quite different from that observed for the other host lattices. The absence of  $P$  and  $R$  branches, the extreme narrow-

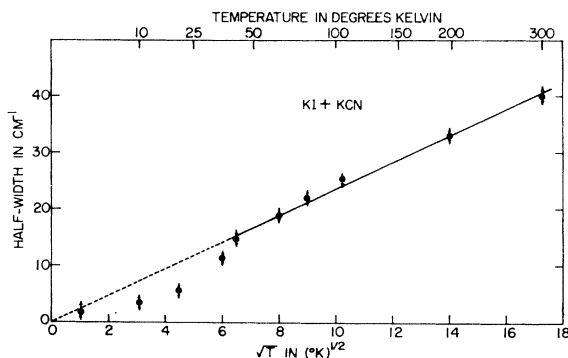


FIG. 16. Half-width of  $\text{CN}^-$  fundamental absorption in  $\text{KI}$  as a function of temperature.

ness of the vibrational transition even at temperatures as high as 80°K, and the fact that the half-width of the band does not follow a  $T^{1/2}$  law indicates that the barrier to rotation in  $\text{NaCl}$  and  $\text{NaBr}$  is extremely high and almost certainly greater than 100  $\text{cm}^{-1}$ . Unfortunately, an accurate estimate of the barrier height cannot be given because a librational satellite for the  $\text{CN}^-$  has not been observed in these two host lattices. From our experimental sensitivity we estimate that any librational transition must be at least 50 to 100 times weaker than the fundamental at low temperatures. This indicates that the  $\text{CN}^-$  sits in a very harmonic potential well so that the  $Q$  branch always dominates the absorption. The origin of the  $T^2$  dependence of the half-width is unknown but it is interesting to note that it is similar to that observed in the near-infrared spectrum of  $U$  centers.<sup>55</sup>

Under uniaxial stress the potential wells in the direction of the stress become deeper and the wells perpendicular to the stress become shallower. A repopulation of the molecules into the deeper wells may occur by the two processes mentioned above. Since the uniaxial stress experiments in this study were carried out below 4°K it is sufficient to raise or lower the wells by only a few degrees Kelvin to observe an alignment. The maximum dichroism was observed for  $[100]$  stress, a smaller dichroism for  $[110]$  stress (with the light propagating parallel to  $[1\bar{1}0]$ ). Hence, we conclude that the equilibrium orientations for the dipoles are the  $\langle 100 \rangle$  directions. The  $T^{-1}$  dependence shows that the dichroism indeed arises through a molecular reorientation under the influence of the external stress. For small stresses the alignment should vary linearly with the applied stress. Departures from this law are observed for stresses smaller than 1 to 1.5  $\text{kg}/\text{mm}^2$ . From this one deduces a zero-stress splitting of  $\sim 0.6 \text{ cm}^{-1}$ . It may be attributed

<sup>50</sup> C. D. Lytle and A. J. Sievers, *Bull. Am. Phys. Soc.* **10**, 616 (1965); C. D. Lytle, M.S. thesis, Cornell University, 1965 (unpublished).

<sup>51</sup> A. J. Sievers, A. A. Maradudin, and S. S. Jaswal, *Phys. Rev.* **138**, A272 (1965).

<sup>52</sup> Even though the primary motion of the molecule at low temperatures is librational they can still reorient very rapidly, see below.

<sup>53</sup> G. Lombardo and R. O. Pohl, *Phys. Rev. Letters* **15**, 291 (1965).

<sup>54</sup> H. S. Sack and C. M. Moriarty, *Solid State Commun.* **3**, 93 (1965). See also Ref. 6.

<sup>55</sup> B. Fritz, in *Proceedings of the Copenhagen Conference on Lattice Dynamics*, edited by R. F. Wallis (Pergamon Press, Inc., New York, 1965), p. 485. D. N. Mirilin and I. I. Reshina, *Fiz. Tverd. Tela* **6**, 945 (1964) [English transl.: *Soviet Phys.—Solid State* **6**, 728 (1964)].

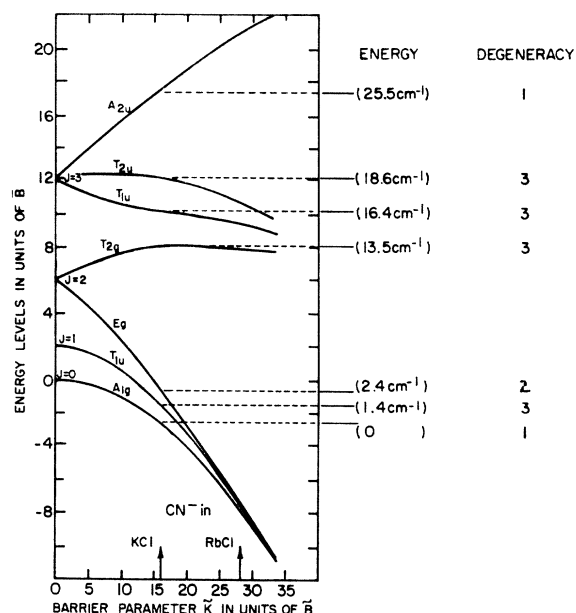


FIG. 17. The energy levels in units of  $\bar{B}$  as a function of the barrier parameter  $\bar{K}/\bar{B}$  for a linear molecule in an octahedral site. After Devonshire, Ref. 58. From this the energy levels for the  $\text{CN}^-$  ions in KCl were calculated. Omitted in this drawing is a threefold degenerate  $T_{1g}(J=4)$  state which approaches the  $T_{2u}(J=3)$  state for large  $\bar{K}$ . For infinite  $K$  the states  $T_{2g}(J=2)$ ,  $T_{1u}$  and  $T_{2u}(J=3)$ , and  $T_{1g}(J=4)$  merge into the 12-fold degenerate first librational state.

to a residual internal stress<sup>56</sup> or to the fact that the ground state of the  $\text{CN}^-$  is split by tunneling (1.4 and 2.4  $\text{cm}^{-1}$ , see the discussion of Devonshire's model in the following).

With  $\langle 100 \rangle$  equilibrium orientations no optical dichroism should be observed for  $[111]$  stress. Hence, the nonvanishing dichroism is surprising. It cannot be caused entirely by inaccuracy in our grinding procedure, which is at most 5°. It is conceivable that the residual internal stresses may tilt the direction of the applied stress for some of the centers so that the stress and the polarized light are no longer perpendicular to each other. There may also be a small probability for the molecules to orient along the  $\langle 111 \rangle$  directions. In that case we would expect for higher potential barriers (smaller tunnel splitting) the dichroism for  $[111]$  stress to be smaller or even to disappear. Finally, and most importantly, the stress dependence of the energy levels is unknown. For these reasons we have not attempted to make a quantitative fit to the data and merely conclude that the alignment is of the Langevin type and the equilibrium orientations of the dipoles are the  $\langle 100 \rangle$

<sup>56</sup> In his work on the  $R$  center Silsbee [R. H. Silsbee, Phys. Rev. 138, A180 (1965)] found similar deviations from a Langevin curve from which he deduced a zero-stress splitting of  $\sim 1.0 \text{ kg mm}^{-2}$ . Sussmann (Ref. 70) used  $3 \text{ kg/mm}^2$  to explain the deviations observed by Känzig [W. Känzig, J. Phys. Chem. Solids 23, 479 (1964)] for the  $O_2^-$  center in KCl.

directions.<sup>57</sup> The latter point will be discussed again in connection with the specific-heat measurements.

The alignment observed in KBr, KI, and RbCl host lattices is similar to that observed in KCl but smaller in magnitude. In all these host lattices the alignment proceeds with a time constant which is much faster than the time constant of our detection system ( $\sim 2 \text{ sec}$ ). Since in the potassium series the barrier height for the  $\text{CN}^-$  is low, both the classical thermal activation process discussed above and the tunneling process have a relaxation time which is shorter than our experimental time constant and it is not possible to decide which process is responsible for the observed alignment. In RbCl the classical process, owing to the high barrier, has a negligible probability at 1.36°K. This implies that the alignment observed in this host lattice is through a tunneling process. From similar arguments the complete lack of alignment observed in NaCl and NaBr between 1.36 and 4.2°K over time periods as long as  $10^8 \text{ sec}$  implies that the tunneling frequency must be smaller than  $10^{-3} \text{ sec}^{-1}$  and the barrier to rotation must be greater than 100  $\text{cm}^{-1}$  [assuming a librational (attempt) frequency of  $10^{12} \text{ sec}^{-1}$ ].

Recently Sack and Moriarty<sup>54</sup> measured the dielectric constant of KCl:CN, KBr:CN, KI:CN and NaCl:CN down to about 2.5°K and in the frequency range 1–100 kc/sec. They found in the potassium series that the dipoles followed the field oscillations but in NaCl they observed no increase in the dielectric constant. Their results are in excellent agreement with the conclusions drawn from our optical data. They found a dipole moment of  $\sim 0.3$  Debye for the  $\text{CN}^-$  in the potassium salts. The small dipole moment accounts for the fact that electric fields of 80 kV/cm cause a change of less than 5% in the  $\text{CN}^-$  infrared band at 2°K.

Now that we have established the equilibrium orientations of the  $\text{CN}^-$  we shall repeat Pauling's calculation with a more realistic potential function in three dimensions and with six potential minima along the  $\langle 100 \rangle$  directions. This will also provide us with quantitative values of the tunnel splitting.

The tunneling probability can be calculated by starting with the librational wave function and then treating the effect of the anharmonic terms in the potential function as a perturbation. For low potential barriers, as in the case for  $\text{CN}^-$  in many alkali halides, a second method may be used. This consists of starting with the free rotor states and then calculating the effect of a crystalline electric field on the  $(2J+1)$ -fold degenerate  $J$ th rotational state. This method has been discussed by Devonshire<sup>58</sup> who calculated the energy levels for a linear molecule in an octahedral site.

<sup>57</sup> For  $[111]$  stress the light was propagated both in  $[112]$  and  $[110]$  directions. Within experimental error the magnitude of the effect was the same. A nonvanishing dichroism was also found for  $[110]$  stress and light propagating in  $[010]$ , with an alignment of 0.35 for a stress of  $\sim 5 \text{ kg mm}^{-2}$ .

<sup>58</sup> A. F. Devonshire, Proc. Roy. Soc. (London) A153, 601 (1936).

The potential function used by Devonshire is<sup>59</sup>

$$\tilde{V}(\theta, \varphi) = (-\tilde{K}/8)(3 - 30 \cos^2\theta + 35 \cos^4\theta + 5 \sin^4\theta \cos 4\varphi),$$

where  $\tilde{K}$  is a constant. For  $\tilde{K}$  positive  $\tilde{V}$  has six minima equal to  $-\tilde{K}$  at the points

$$\theta = 0 \text{ or } \pi; \quad \theta = \pi/2, \quad \varphi = 0, \quad \pm \frac{1}{2}\pi, \text{ or } \pi,$$

which correspond to the six  $\langle 100 \rangle$  directions in the crystal. The potential maxima lie along

$$\theta = \cos^{-1}(\pm 1/\sqrt{3}), \quad \varphi = \pm \pi/4 \text{ or } \pm 3\pi/4,$$

which are the eight  $\langle 111 \rangle$  directions in the crystal. Two wells lying in adjacent  $\langle 100 \rangle$  directions are separated by a potential barrier of  $1.25 \tilde{K}$  in the  $\langle 100 \rangle$  directions.

Devonshire has given the energy eigenvalues of the Schrödinger equation for the potential  $\tilde{V}(\theta, \varphi)$ . For  $\tilde{K} = 0$  the solutions reduce to the free-rotor energy levels. For  $\tilde{K} \neq 0$ , the degeneracy of the rotational energy levels is partly removed. The energy levels for  $J = 0, 1, 2, 3$  have been plotted in units of the rotational constant  $\tilde{B}$  as a function of  $\tilde{K}/\tilde{B}$  and are shown in Fig. 17. For high positive values of the barrier parameter,  $\tilde{K}$ , the  $A_{1g}(J=0)$ ,  $T_{1u}(J=1)$ , and  $E_g(J=2)$  states have very nearly the same energy. In the high-barrier limit they present a sixfold degenerate librational ground state as should be the case for the 6 minima potential considered. The  $T_{2g}(J=2)$  state will represent the first excited librational state.

Using the well-known electric dipole selection rules<sup>60</sup> the value of the barrier parameter  $\tilde{K}$  can be determined from the observed splitting of the librational sum satellite  $T_{1u}(J=1) \rightarrow T_{2g}(J=2)$ . Note that all transitions occur simultaneously with a change  $\Delta v = +1$  in vibrational quantum number of the C-N stretching vibration. For a splitting of  $12 \text{ cm}^{-1}$  it follows that  $\tilde{K} = 16\tilde{B} = 20 \text{ cm}^{-1}$ . From this a barrier height in  $\langle 110 \rangle$  is determined to  $\tilde{V}_0 = 1.25 \tilde{K} = 25 \text{ cm}^{-1}$ . It is gratifying to find that the sophisticated Devonshire model yields a barrier height in very close agreement with the one determined from the simple two-well Pauling potential, for which  $\tilde{V}_0 = 24 \text{ cm}^{-1}$  was found. In Fig. 17 the level scheme for  $\text{CN}^-$  in the potassium halides is shown with the appropriate energies. Sum transitions from  $A_{1g}(J=0) \rightarrow T_{1u}(J=3)$  and  $T_{2u}(J=3)$  with  $\Delta J = 3$  should be less likely. Transitions from  $E_g(J=2)$  to  $T_{1u}$  and  $T_{2u}(J=3)$  should be possible if  $E_g$  is thermally populated. These transitions may be partly responsible for the observed breadth of the sum satellite. Note,

<sup>59</sup> This is the lowest order surface harmonic of octahedral symmetry. Such a potential is obtained by considering the electrostatic field due to an octahedron of charges and is often used to study the splitting of the energy levels of paramagnetic atoms in an octahedral field. See also Ref. 60.

<sup>60</sup> See for example M. Tinkham, *Group Theory and Quantum Mechanics* (McGraw-Hill Book Company, New York, 1964). See also Ref. 41. The intensities of the different transitions listed in the text depend on the magnitude of the coefficients in the expansion of the wave functions corresponding to the various energy states in the Devonshire model. These coefficients have as yet not been determined as a function of  $\tilde{K}$ . These are presently under investigation.

however, that  $T_{1u}(J=3)$  and  $T_{2u}(J=3)$  lie so close to the barrier in contrast to  $T_{2g}(J=2)$  that they are more appropriately called rotor states and hence would have a smaller probability of mixing with the librational  $E_g(J=2)$  state.<sup>60</sup> The optical transitions giving rise to the strong central line in the absorption spectrum at low temperatures are  $A_{1g}(J=0) \rightarrow T_{1u}(J=1)$  and the inverse,  $T_{1u}(J=1) \rightarrow A_{1g}(J=0)$ , [at somewhat higher temperatures also  $T_{1u}(J=1) \leftrightarrow E_g(J=2)$  according to the thermal population of these states]. Note that these transitions are not, strictly speaking,  $Q$  transitions. The  $Q$  transitions are parity forbidden. The two transitions  $T_{1u}(J=1) \leftrightarrow A_{1g}(J=0)$ , different by  $2.8 \text{ cm}^{-1}$  could not be resolved except perhaps in KI (at  $2064.5 \text{ cm}^{-1}$  in Fig. 7) despite adequate instrumental resolution ( $0.6 \text{ cm}^{-1}$ ). The width of the observed band is, however,  $2.5 \text{ cm}^{-1}$ . We shall return to this important point in the summary of the IR results. The difference satellite arises above  $10^\circ\text{K}$  because of thermal population of the  $T_{2g}(J=2)$  and of the  $T_{1u}(J=3)$  and possibly the  $T_{2u}(J=3)$  states. The selection rules predict a difference transition  $T_{2g}(J=2) \rightarrow T_{1u}(J=1)$  at  $12 \text{ cm}^{-1}$ , plus transitions  $T_{1u}(J=3) \rightarrow T_{2g}(J=2)$  at  $2.9 \text{ cm}^{-1}$  and  $T_{2u}(J=3) \rightarrow T_{2g}(J=2)$  at  $5.1 \text{ cm}^{-1}$ . What we observe is one broad band separated by less than the separation of the sum satellite.

Similarly, the librational frequency of  $19 \text{ cm}^{-1}$  in  $\text{RbCl}$  yields  $\tilde{K} \approx 28\tilde{B} \approx 35 \text{ cm}^{-1}$ . The  $T_{1u}$  and  $E_g$  tunnel levels are expected to lie  $0.625$  and  $0.75 \text{ cm}^{-1}$ , respectively above the  $A_{1g}$  state. This would predict a difference satellite  $1.2 \text{ cm}^{-1}$  away which was again not resolved. However, the experimentally observed width of the central line in  $\text{RbCl}$  is about  $1 \text{ cm}^{-1}$ , i.e., much smaller than that observed in  $\text{KCl}$ , and is qualitatively consistent with our supposition that the width arises from unresolved tunneling transitions.

### C. Summary of IR Results

The IR measurements on  $\text{CN}^-$  in  $\text{KCl}$ ,  $\text{KBr}$ ,  $\text{KI}$  and  $\text{RbCl}$  have shown that at high temperatures the molecules can rotate freely in the lattice. At low temperatures the molecules perform librational motions with a frequency of  $11$  to  $12 \text{ cm}^{-1}$  in the potassium halides and about  $19 \text{ cm}^{-1}$  in  $\text{RbCl}$ . In addition uniaxial-stress measurements show that in these host lattices the  $\text{CN}^-$  can reorient down to the lowest temperature of our measurements ( $1.36^\circ\text{K}$ ), the minima in the potential function being the  $\langle 100 \rangle$  directions.

In  $\text{NaCl}$  and  $\text{NaBr}$  the  $\text{CN}^-$  is "locked-in" at low temperatures and the barrier hindering rotation is estimated to be greater than  $100 \text{ cm}^{-1}$ .

Finally, the energy levels of the  $\text{CN}^-$  in a six-well potential have been quantitatively considered for the potassium halides and  $\text{RbCl}$  in terms of the Devonshire model. This model can explain the gross features of the IR data but predicts tunneling transitions which were not observed in our optical measurements.

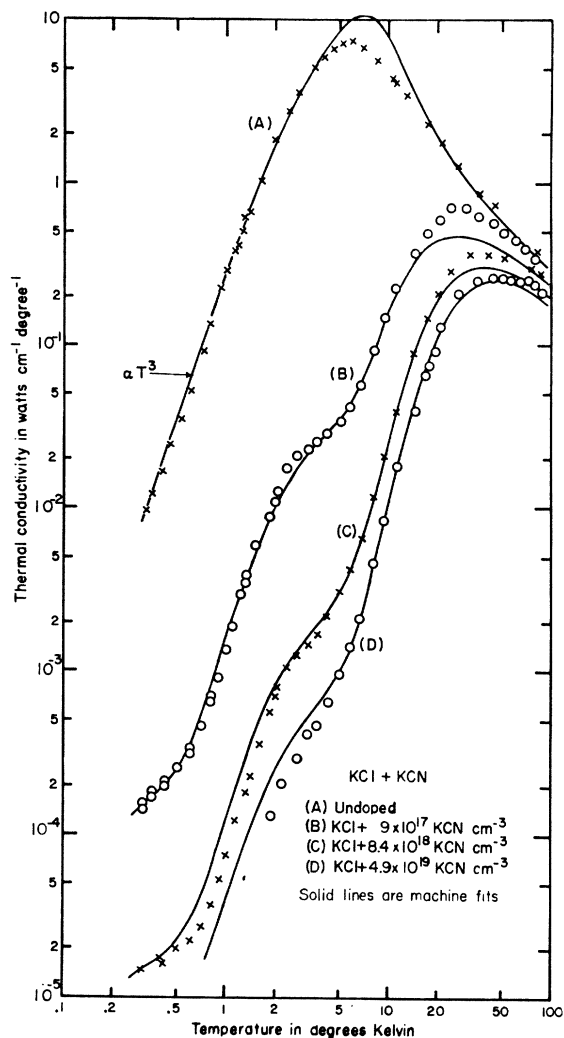


FIG. 18. Thermal conductivity of KCl:CN.  $\text{CN}^-$  concentrations are: (A) undoped, (B)  $9 \times 10^{17} \text{ cm}^{-3}$ , (C)  $8.4 \times 10^{18} \text{ cm}^{-3}$ , (D)  $4.9 \times 10^{19} \text{ cm}^{-3}$ .  $\text{NCO}^-$  concentrations are  $1-3 \times 10^{18} \text{ cm}^{-3}$ . Solid lines are machine fits as described in text.

The following questions may therefore be legitimately asked:

(1) Is the Devonshire model correct for the  $\text{CN}^-$ ? If so why were the tunneling transitions in the IR data not resolved?

(2) Can one account for the fact that the rotational fine structure of the  $P$  and  $R$  branches at high temperatures is not resolved?

These questions can be satisfactorily answered by thermal conductivity and specific-heat measurements. We have measured the thermal conductivity of KCl, KBr, and NaCl containing  $\text{CN}^-$  and the specific heat of KCl:CN. The result of these investigations is the subject of the next section.

## VI. THERMAL CONDUCTIVITY AND SPECIFIC-HEAT RESULTS

To answer the questions posed in the preceding section we have measured the thermal conductivity to study the phonon interactions in CN-doped crystals. In contrast to optical spectroscopy, phonon spectroscopy via thermal conductivity is a broad-band technique. In lieu of a phonon monochromator one passes essentially a blackbody distribution of phonons down the crystal by means of a thermal gradient. The thermal conductivity is the transmission of this spectrum by the crystal integrated over all phonon frequencies. To unfold the phonon-scattering rates a method of curve-fitting is used that has been previously described and tested.<sup>61,62</sup> Limitations of the simple theory in the presence of strong normal processes have been recently discussed by Berman and Brock<sup>63</sup> and Thacher.<sup>64</sup>

### A. Data and Curve Fitting for KCl:CN

The thermal conductivity of the system KCl:CN is shown in Fig. 18. Striking features of the doped crystals are the great reduction in conductivity and the distinct depressions in the curves at  $0.6^\circ$  and  $7^\circ\text{K}$ . From this it follows that certain phonon frequencies interact very strongly with the  $\text{CN}^-$ . It is these resonance frequencies that we wish to correlate with infrared-spectroscopic data. For a quantitative analysis of the scattering we use the Debye model of the thermal conductivity. Then the thermal conductivity  $K(T)$  is given by the following equation:

$$K(T) = 1/2\pi^2 v \int_0^{\omega_D} \tau(T, \omega) \frac{\hbar^2 \omega^4}{kT^2} \frac{e^{\hbar\omega/kT}}{(e^{\hbar\omega/kT} - 1)^2} d\omega. \quad (7)$$

Here,  $v$  is the sound velocity,  $\omega_D$  is the Debye cutoff frequency, and  $\tau(T, \omega)$  is the combined relaxation time given by

$$\tau^{-1}(T, \omega) = \sum_j \tau_j^{-1}(T, \omega).$$

In this equation  $\tau_j^{-1}(T, \omega)$  is the relaxation rate of the  $j$ th scattering mechanism.

The combined relaxation rate giving the best fit to the pure KCl data is

$$\tau_p^{-1} = 4.9 \times 10^5 \text{ sec}^{-1} + 6.07 \times 10^{-44} \text{ sec}^3 \omega^4 + 3.64 \times 10^{-18} \text{ sec deg}^{-1} T \omega^2 e^{-40^\circ\text{K}/T}. \quad (8)$$

The individual scattering terms are boundary, isotope, and umklapp, respectively, and their origin is discussed in Ref. 65.<sup>66</sup> The accuracy of the pure-crystal fit

<sup>61</sup> J. Callaway, Phys. Rev. **113**, 1046 (1959).

<sup>62</sup> R. O. Pohl, Z. Physik **176**, 358 (1963).

<sup>63</sup> R. Berman and J. C. F. Brock, Proc. Roy. Soc. (London) **A289**, 46 (1965).

<sup>64</sup> P. D. Thacher, Ph.D. thesis, Cornell University, 1965 (unpublished).

<sup>65</sup> C. T. Walker and R. O. Pohl, Phys. Rev. **131**, 1433 (1965).

<sup>66</sup> The average sound velocity used here is calculated from the Debye temperature,  $\Theta$ , using the equation

$$v = \Theta k^{-1} (6\pi^2 n)^{-1/3} = 2.5 \times 10^5 \text{ cm/sec},$$

where  $n$  is the number of atoms per unit volume, not the number of KCl molecules as was used in Ref. 65.

is more than adequate since in fitting the doped crystals one has to add a relaxation rate that completely dominates the pure-crystal rate except at high temperatures.

The doped crystals were fit with the following relaxation rate that had previously been used to fit KCl:CN<sup>-</sup> data<sup>7</sup>:

$$\tau^{-1} = \tau_p^{-1} + N \left[ \frac{D_1 \omega_1^2 \omega^2}{(\omega_1^2 - \omega^2)^2 + \Gamma_1^2 \omega_1^2} + \frac{D_2 \omega_2^2 \omega^2}{(\omega_2^2 - \omega^2)^2 + \Gamma_2^2 \omega_2^2} \right]. \quad (9)$$

The scattering rate for each depression had to have a resonance form falling off rapidly on both sides of the resonance frequency. The expression used satisfies these requirements and in addition has a very plausible form analogous to the scattering rate of photons by atomic states. A problem similar to ours has been treated by Griffin and Carruthers.<sup>67</sup> They calculated the scattering rate by donor electrons in germanium and obtained an expression similar to that used here except for the frequency dependence of the numerator which comes from a detailed knowledge of the electron-phonon interaction. Calculations of the scattering of phonons by molecules have been made by Wagner using both perturbation theory<sup>68</sup> and Green's-function techniques.<sup>69</sup> His scattering rates were of a resonance type not greatly different from that used in this paper. However, sufficient details of the phonon-molecule interaction were not included and so comparison with experiment was not possible. It was recently suggested by Sussmann<sup>70</sup> that tunneling induced by single phonons could be responsible for the phonon scattering by molecules. His calculation was based on scattering between states split by the residual internal strain and he found a phonon-relaxation rate proportional to the phonon frequency in contrast to our results.

At present it appears that there is no firm theoretical basis for the use of Eq. (9). We therefore merely state that it fits the data well and proceed to use it in determining the resonance frequencies.

The constants  $D_1 = 1.16 \times 10^{-10} \text{ cm}^3 \text{ sec}^{-1}$ ,  $D_2 = 7.5 \times 10^{-10} \text{ cm}^3 \text{ sec}^{-1}$ ,  $\Gamma_1 = 0$ ,  $\Gamma_2 = 0$ ,  $\omega_1 = 3 \times 10^{11} \text{ sec}^{-1}$  ( $\tilde{\nu}_1 = 1.6 \text{ cm}^{-1}$ ), and  $\omega_2 = 3.54 \times 10^{12} \text{ sec}^{-1}$  ( $\tilde{\nu}_2 = 18 \text{ cm}^{-1}$ ) were chosen to give the best fit to the data for sample (B).  $N$  was the optically determined CN<sup>-</sup> concentration in this crystal.<sup>71</sup> For samples (C) and (D) effective values of  $N$  were determined to give good agreement between the machine fit and the data in the temperature range 5° to 20°K. The scaling of the strength of the phonon scattering with CN<sup>-</sup> concentra-

tion is demonstrated by the effective values of  $N$  for curves (C) and (D),  $11.6 \times 10^{18} \text{ cm}^{-3}$  and  $3.7 \times 10^{19} \text{ cm}^{-3}$ , respectively, which agree within experimental error with the optically determined CN<sup>-</sup> concentration,  $8.4 \times 10^{18} \text{ cm}^{-3}$  and  $4.9 \times 10^{19} \text{ cm}^{-3}$ , respectively. The phonon scattering does not scale with NCO<sup>-</sup> concentration which varies by only a factor of 3 between samples (B) and (D). From this together with the fact that the infrared spectra of NCO<sup>-</sup> consist of very narrow lines we conclude that NCO<sup>-</sup> does not scatter phonons.

### B. Origin of the Resonance Frequencies in KCl:CN

A very plausible origin for the phonon resonance frequencies  $\omega_1$  and  $\omega_2$  can be seen from the energy-level diagram of CN<sup>-</sup> in KCl, Fig. 17.

The resonance energy  $\hbar\omega_1 (1.6 \text{ cm}^{-1})$  is very nearly equal to the tunneling splitting. This suggests that the low-temperature depression in the thermal-conductivity curves is caused by a resonance phonon absorption in which the CN<sup>-</sup> is excited from the ground state,  $A_{1g}$ , to one or both of the next two levels, namely  $T_{1u}$  ( $1.4 \text{ cm}^{-1}$ ) or  $E_g$  ( $2.4 \text{ cm}^{-1}$ ). Subsequent de-excitation of the molecule would result in the emission of a phonon of the same energy but in a random direction. Thus the over-all process would add to the thermal resistance. Such a strong phonon interaction would cause appreciable broadening of levels  $T_{1u}$  and  $E_g$  and could explain why the tunneling splitting was not resolved in the infrared spectra. It is not possible to say that  $A_{1g} \rightarrow T_{1u}$  is favored over  $A_{1g} \rightarrow E_g$  or vice-versa since the energy levels are not that accurately known and in addition the thermal conductivity data cannot be fit that precisely. The  $T_{1u} \rightarrow E_g$  transition, however, cannot have an appreciable effect on the thermal conductivity since in order to populate  $T_{1u}$ , one has to go to temperatures so high that the dominant phonons have energies considerably larger than the separation of  $T_{1u}$  and  $E_g$ .<sup>72</sup>

The second dip in the thermal conductivity requires a phonon resonance energy of  $\tilde{\nu}_2 = 18 \text{ cm}^{-1}$  which is about equal to the positions of the  $T_{1u}$  ( $16.4 \text{ cm}^{-1}$ ) and  $T_{2u}$  ( $18.6 \text{ cm}^{-1}$ ) levels. We conclude that there is a strong phonon coupling between these states and the tunneling states. Transitions to the librational level  $T_{2g}$  ( $13.5 \text{ cm}^{-1}$ ) are not observed in the thermal conductivity. This is in agreement with the low-temperature infrared spectra which indicate that the librational level is not greatly broadened. Furthermore it appears generally true that librational levels do not scatter phonons strongly since NCO<sup>-</sup> in KCl which does not affect the thermal conductivity has librational levels spaced at about  $4 \text{ cm}^{-1}$ .<sup>73</sup>

<sup>67</sup> A. Griffin and P. Carruthers, Phys. Rev. **131**, 1976 (1963).

<sup>68</sup> M. Wagner, Phys. Rev. **131**, 1443 (1963).

<sup>69</sup> M. Wagner, Phys. Rev. **131**, 2520 (1963); **133**, A750 (1962).

<sup>70</sup> J. A. Sussmann, Phys. Kondensierten Materie **2**, 479 (1964).

<sup>71</sup> The damping terms,  $\Gamma_1$  and  $\Gamma_2$ , could be as large as  $0.4\omega_1$  and  $0.4\omega_2$ , respectively without making the fit to the data noticeably poorer. This is because the damping affects only a small fraction of the phonons.

<sup>72</sup> The dominant phonons in carrying the heat current at low temperatures have the energy  $\hbar\omega_M \approx 4kT$ .  $\omega_M$  is the frequency for which the integrand, apart from  $\tau$ , in the thermal-conductivity integral is a maximum.

<sup>73</sup> Note, however, Ref. 24. For a discussion of the phonon interaction with librational states we refer to Ref. 6.

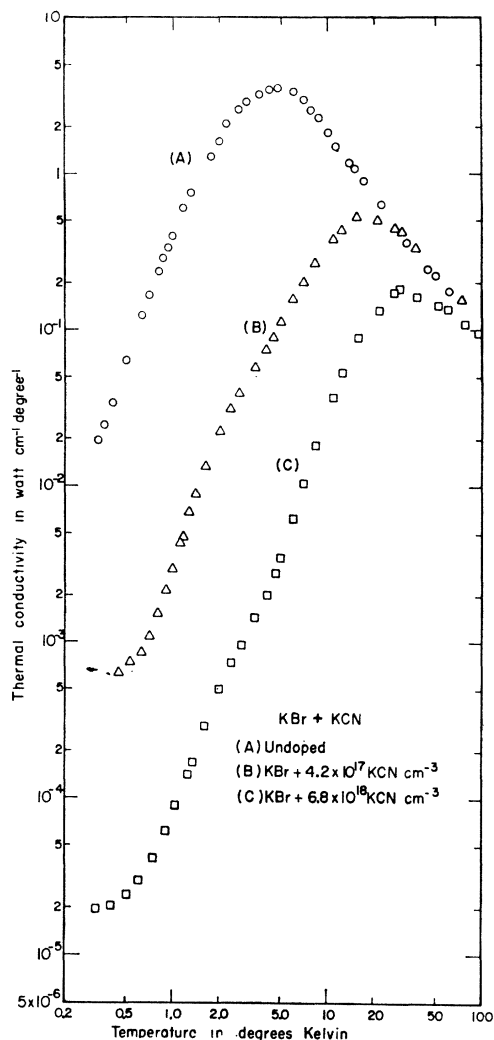


FIG. 19. Thermal conductivity of KBr:CN.  $\text{CN}^-$  concentrations are A—undoped, B— $4.2 \times 10^{17} \text{ cm}^{-3}$ , C— $6.8 \times 10^{18} \text{ cm}^{-3}$ ,  $\text{NCO}^-$  concentrations are B— $3 \times 10^{18} \text{ cm}^{-3}$  and C— $7 \times 10^{18} \text{ cm}^{-3}$ .

No scattering by transitions to higher energy levels beginning at  $25.5 \text{ cm}^{-1}$  is reflected in the thermal conductivity. There are several reasons for this. Some transitions will be eliminated by selection rules on the matrix elements. Secondly, there may be a mismatch between the energies of the allowed transitions and the energies of the dominant phonons available at a particular temperature. This combined with population considerations for the  $\text{CN}^-$  levels could rule out the possibility of seeing dips at higher temperatures. Finally, the umklapp scattering rate increases exponentially with temperature and eventually dominates all other scattering mechanisms.

We should note that the  $T_{1u}$  ( $16.4 \text{ cm}^{-1}$ ) and  $T_{2u}$  ( $18.6 \text{ cm}^{-1}$ ) levels, which we believe to be responsible for the depression in the thermal conductivity at  $6^\circ\text{K}$ , lie just about at the top of the potential barrier ( $19 \text{ cm}^{-1}$

above  $A_{1g}$ ) and hence are the first rotational states of the molecule. Phonon-induced transitions between higher rotational states although not observed in the thermal conductivity, would account for the missing fine structure in the high temperature infrared spectra.

### C. Thermal Conductivity of KBr:CN, KI:CN, and NaCl:CN

Figure 19 shows that the phonon scattering by  $\text{CN}^-$  in KBr is very nearly the same as in KCl. The only difference is that the  $6^\circ\text{K}$  resonance in KBr:CN is considerably broader. Here again the positions of the resonances can be explained in the same way as for KCl:CN since the infrared spectra of KBr:CN and KCl:CN are virtually the same.

The thermal conductivity of one KI crystal containing  $5 \times 10^{19} \text{ CN}^- \text{ cm}^{-3}$  was measured between  $0.3^\circ$  and  $1.5^\circ\text{K}$ . The data points were almost identical to those in the lower portion of curve (C) in Fig. 19. Since the  $\text{CN}^-$  concentration in the KI crystal was about 5 times that in sample (C) we conclude that the scattering is weaker in KI but otherwise the same for small  $\omega$  ( $1.6 \times 10^{11} - 8 \times 10^{11} \text{ rad sec}^{-1}$ ). The weaker coupling to the phonons as reflected in the thermal conductivity is consistent with the optical data for  $\text{CN}^-$  in KI where there are the first indications of the resolution of the tunneling splitting.

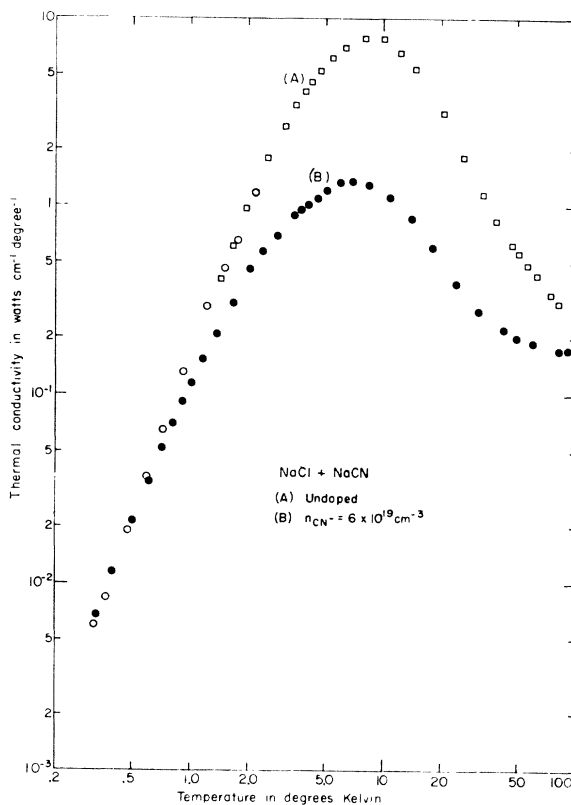


FIG. 20. Thermal conductivity of NaCl:CN. A—undoped, B has  $6 \times 10^{19} \text{ CN}^- \text{ cm}^{-3}$  and  $5 \times 10^{17} \text{ NCO}^- \text{ cm}^{-3}$ .



In the three previous systems two resonances in the phonon scattering can be explained with the energy level diagram based on spectroscopic data. One of the phonon resonance energies matches the tunneling splitting of the  $\text{CN}^-$ . The other matches the energy difference between the ground state and rotational states lying at the top of the potential well. To test the generality of this model  $\text{CN}^-$  in  $\text{NaCl}$  was studied. Here the infrared spectra show that the  $\text{CN}^-$  is frozen in. There is no tunneling splitting and the rotational states lie at least  $100\text{ cm}^{-1}$  above the ground state. We would expect, therefore, no effect on the thermal conductivity except perhaps at high temperatures. Figure 20 shows the  $\text{NaCl}:\text{CN}$  thermal conductivity results. Indeed at low temperatures the  $\text{CN}^-$  has no effect. The depression at  $40^\circ\text{K}$  may be caused by scattering of the  $\text{CN}^-$  both as a molecule and as a point defect. Similar high-temperature depressions have been observed in the thermal conductivity of crystals containing about the same concentration of monatomic defects.<sup>65</sup> Assuming, however, that the scattering is caused by rotational states of the  $\text{CN}^-$  lying at the top of the potential barrier we estimate the barrier height to be  $140\text{ cm}^{-1}$  from the position of the dip in the thermal conductivity.<sup>72</sup> This is in agreement with infrared data discussed previously which place the barrier above  $100\text{ cm}^{-1}$ .

#### D. Specific Heat of $\text{KCl}:\text{CN}$

Direct evidence for the existence of the tunneling splitting can be obtained with specific heat measure-

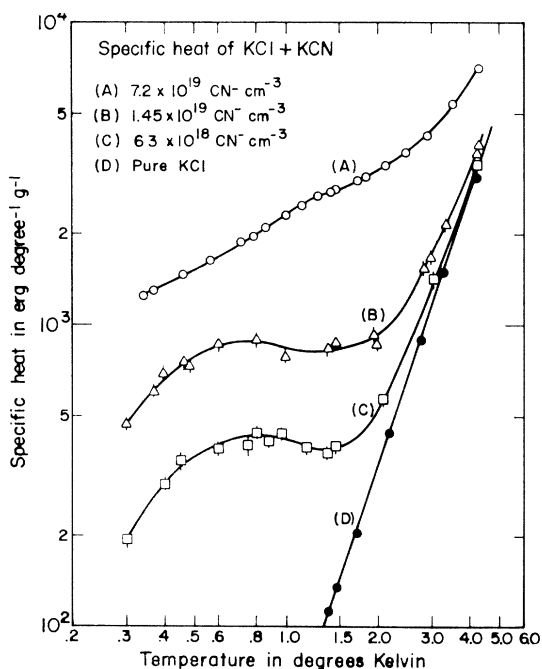


FIG. 21. Specific heat  $c_v$  of  $\text{KCl}:\text{CN}$ .  $\text{CN}^-$  concentrations are A— $7.2 \times 10^{19}\text{ cm}^{-3}$ , B— $1.5 \times 10^{19}\text{ cm}^{-3}$ , C— $6.3 \times 10^{18}\text{ cm}^{-3}$ .  $\text{NCO}^-$  concentrations are (A)  $2.5 \times 10^{19}\text{ cm}^{-3}$ , (B)  $2 \times 10^{18}\text{ cm}^{-3}$ , and (C)  $1.6 \times 10^{18}\text{ cm}^{-3}$ .

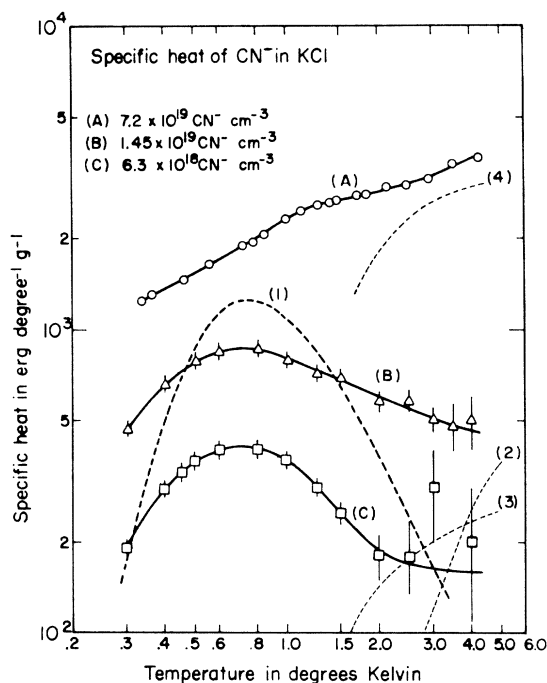


FIG. 22. Curves (A), (B), and (C) are the specific heat of  $\text{KCl}:\text{CN}$  with  $\text{KCl}$  lattice specific heat subtracted. Same crystals as in Fig. 21. Curve 1 is the Schottky anomaly expected for  $\text{CN}^-$  tunneling levels, curve 2 is the approximate contribution of the higher  $\text{CN}^-$  levels, and curve 3 is the approximate contribution of the  $\text{NCO}^-$  librational levels, all calculated for crystal (B). Curve 4 is the approximate  $\text{NCO}^-$  contribution in crystal (A). The specific heat of the  $\text{NCO}^-$  librational levels, spaced at  $4\text{ cm}^{-1}$ , is that of a two-dimensional harmonic oscillator.

ments. The tunneling states should produce a Schottky-type anomaly similar to that found in paramagnetic salts having a ground state which is split by the crystalline field.<sup>74</sup> Ignoring for the moment all levels but the tunneling levels the specific heat may be written

$$c_v = N \frac{\partial}{\partial T} \left( \frac{g_1 \Delta_1 e^{-\Delta_1/kT} + g_2 \Delta_2 e^{-\Delta_2/kT}}{g_0 + g_1 e^{-\Delta_1/kT} + g_2 e^{-\Delta_2/kT}} \right). \quad (10)$$

Here 0, 1 and 2 refer to the  $A_{1g}$ ,  $T_{1u}$ , and  $E_g$  levels, respectively,  $\Delta_i$  is the energy of the  $i$ th level above the ground state  $A_{1g}$ ,  $g_i$  is the degeneracy of the  $i$ th level, and  $N$  is the number of molecules. From this expression the entropy may be calculated and particularly the change in entropy in going from a temperature in which all of the molecules are in the ground state to one in which there is an equal probability for the molecule to be in any one of the 6 states. From statistical mechanics this change in entropy is  $\Delta S = k \ln 6$  per molecule and is independent of how the levels are spaced.

The measured specific heat of  $\text{KCl}:\text{CN}$  is shown in Fig. 21. This graph shows dramatically the size of the anomaly relative to the size of the lattice specific heat

<sup>74</sup> H. M. Rosenberg, *Low Temperature Solid State Physics* (Oxford University Press, Oxford, 1963).

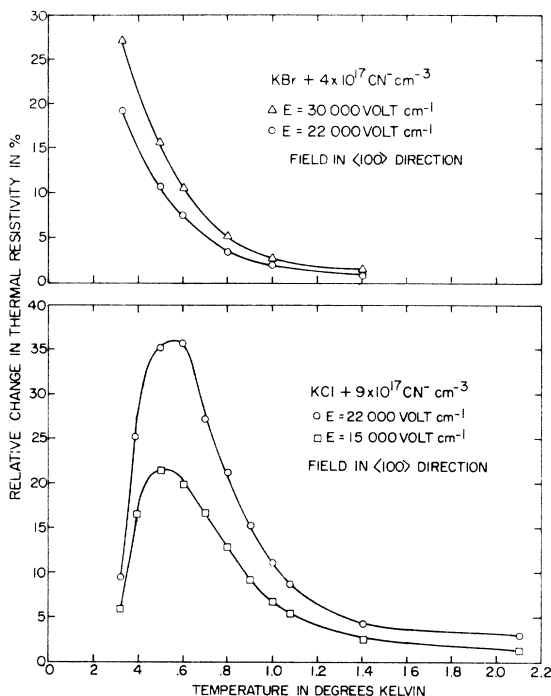


FIG. 23. Relative change in thermal resistivity on applying an electric field  $E$ . The KBr crystal had  $4 \times 10^{17} \text{ CN}^- \text{ cm}^{-3}$  and  $3 \times 10^{18} \text{ NCO}^- \text{ cm}^{-3}$ . The KCl crystal had  $9 \times 10^{17} \text{ CN}^- \text{ cm}^{-3}$  and  $10^{18} \text{ NCO}^- \text{ cm}^{-3}$ .

[Curve (D)] but in order to analyze the anomaly the lattice specific heat must be subtracted (Fig. 22). The theoretical curve (1), calculated from Eq. (10) using the energies and degeneracies from Fig. 17, is the expected Schottky specific heat for sample (B). Curves (B) and (C) exhibit the same shape below  $1.5^\circ\text{K}$  indicating that the level spacing is in reasonable agreement with the prediction but both curves are broader than the calculated curve. We attribute this broadening to the residual strain in the crystal that was previously discussed.

For a quantitative comparison between theory and experiment the change in entropy  $\Delta S$  was determined by graphical integration of the measured  $c_v/T$  curves between  $0.3^\circ$  and  $4.2^\circ\text{K}$ .

$$\Delta S_B = N_B k \ln(6.3 \pm 0.6)$$

$$\Delta S_C = N_C k \ln(5.6 \pm 0.6).$$

This demonstrates not only that the specific heat anomaly scales with the  $\text{CN}^-$  concentration but also that the tunneling levels in fact consist of a total of 6 states as expected in the case of six (100) equilibrium orientations.

Curve (A),  $N = 7.2 \times 10^{19} \text{ cm}^{-3}$ , does not show the expected maximum in the specific heat at  $0.7^\circ\text{K}$ . Its shape is somewhat similar to the specific heat measured on  $\text{KCl:OH}^-$ .<sup>75</sup> In our case, however, it is not possible to

<sup>75</sup> I. Shepherd and G. Feher, Phys. Rev. Letters **15**, 194 (1965).

explain this as a dipole-dipole interaction leading to antiferroelectric ordering of the  $\text{CN}^-$  dipoles.<sup>76</sup> With the small  $\text{CN}^-$  dipole moment and for this concentration the critical temperature  $T_c$  would be about  $0.07^\circ\text{K}$  for a uniform distribution of the ions.<sup>77</sup> Unless the  $\text{CN}^-$  ions were nonrandom in crystal (A) we must assume that some other defects were producing a change in the energy levels of the  $\text{CN}^-$  ions. It should be noted that in this sample (compared to the samples of the IR and the thermal conductivity studies) the  $\text{NCO}^-$  concentration was 10 times higher,  $N_{\text{NCO}} = 2.5 \times 10^{19} \text{ cm}^{-3}$ . The librational energy levels of the  $\text{NCO}^-$  ions and the higher states of the  $\text{CN}^-$  ion (see Fig. 17) certainly account for the rise in specific heat above  $2^\circ\text{K}$  observed in all three samples. For details we refer to the caption of Fig. 22.

### E. Influence of an Electric Field on the Thermal Conductivity

An electric field should change the energy levels of the  $\text{CN}^-$  ion. This effect turned out to be too small to be detected in the infrared. There is, however, a large effect on the thermal conductivity, as shown in Fig. 23. There the change in thermal resistivity on applying an electric field divided by the zero-field resistivity is plotted versus temperature. The curves are similar for KCl and KBr except that in KBr the curves are shifted to lower temperatures. In order to understand this effect let us first assume that the electric field increases the ground-state splitting of  $1.6 \text{ cm}^{-1}$  which was extracted from the thermal-conductivity data [Fig. 18 and Eq. (9)]. We computed the conductivity for a splitting of  $1.9 \text{ cm}^{-1}$  and found a change quite similar to the effect measured for KCl. Furthermore, assuming that this additional splitting ( $0.3 \text{ cm}^{-1}$ ) is simply  $\Delta = 2\mu_{\text{CN}^-} \times E$  we determine for  $E = 30 \text{ kV/cm}$ ,  $\mu_{\text{CN}^-} \sim 0.3 \text{ D}$ , in agreement with the accepted value.

A comparison of the KCl and KBr data shows that such a simple picture is inadequate.<sup>78</sup> Instead one must calculate the field dependence of the energy levels (Fig. 17) and it is conceivable that this would be different for the two host lattices. It appears that experiments of this kind can provide a better understanding of the lowest energy states of molecules in solids.

## VII. SUMMARY AND CONCLUSIONS

The three different experimental methods described above have resulted in a detailed picture of the rotational degrees of freedom of the molecular impurity  $\text{CN}^-$  in a variety of alkali halide host lattices. This picture is in very good agreement with a model proposed by Pauling as refined by Devonshire. The po-

<sup>76</sup> R. Brout, Phys. Rev. Letters **14**, 175 (1965).

<sup>77</sup> W. Känzig, H. R. Hart, and J. S. Roberts, Phys. Rev. Letters **13**, 543 (1964).

<sup>78</sup> Note, however, the high  $\text{NCO}^-$  concentration in the KBr sample.

tential barrier allows free rotation above 60°K in the potassium salts and above 150°K in the rubidium salt. In the sodium salts finally even at 300°K no free rotation is observed. At temperatures sufficiently below the ones mentioned the molecules perform librational (oscillatory) motions, and at intermediate temperatures the motion can be described with the classical picture of hindered rotation. The librational levels are split due to tunneling, and specific-heat measurements show that this tunnel splitting is in complete agreement with the theory. It was also found that the rotational and the tunneling states couple strongly to the phonons, whereas the librational states do not. The phonon-scattering cross sections have a Lorentzian resonance form. The phonon-molecule interaction is assumed to be through stress coupling which has been shown to be large from stress-induced alignment experiments.

In the KBr and KI host lattices an additional center-of-mass motion of the  $\text{CN}^-$  ions appears likely.

This type of motion had not been considered in the Pauling model. On the other hand a central instability should certainly be expected for cavities considerably larger than the impurity ion. We must therefore ask whether the Pauling model describes the general case of molecular degrees of freedom in solids, or whether the  $\text{CN}^-$  ion is an exception. It is the purpose of the following paper to answer this question.

#### ACKNOWLEDGMENTS

The authors thank Professor R. O. Pohl for his guidance and encouragement throughout the course of this investigation. We thank Professor J. A. Krumhansl, Professor H. Sack, and Professor A. Sievers for valuable discussions. P. Tam was of great help with the computer programming.

The financial support of U. S. Atomic Energy Commission and Advanced Research Projects Agency is gratefully acknowledged.

## Rotational Degrees of Freedom of Molecules in Solids. II. The Nitrite Ion in Alkali Halides

V. NARAYANAMURTI,\* W. D. SEWARD,† AND R. O. POHL

*Laboratory of Atomic and Solid State Physics, Cornell University, Ithaca, New York*

(Received 28 January 1966)

In continuation of the work described in the preceding paper we have studied a defect with three different principal axes of inertia, namely the  $\text{NO}_2^-$  ion. In KCl and KBr, the energy levels corresponding to free rotation, libration, and tunneling have been found. They have been analyzed in the same manner as in the preceding paper. Very different potential barriers for the three different axes of rotation have been found. Strong phonon scattering is again observed in connection with the states of free rotation and of tunneling. In NaCl the ion is frozen in even at room temperature and is only librating. In KI further evidence is found that the  $\text{NO}_2^-$  ion does occupy an off-center position. Consequently the molecule can perform not only rotational, but also translational motion, i.e., its potential is considerably more complex than the Pauling-Devonshire potential. Hence the KI: $\text{NO}_2$  system seems to present the most general case of motion of molecules in solid solution. From the fine structure of the near infrared spectrum of KI: $\text{NO}_2$  we have found all the impurity modes detected so far by different techniques, which shows that this type of spectroscopy is a very useful tool for the study of impurity modes. We suggest further that some of these impurity modes are librational motions.

### I. INTRODUCTION

IN the preceding article<sup>1</sup> we showed that infrared and thermal measurements combined gave a complete picture of the low-lying energy levels of the cyanide ion in various alkali halides. In the present paper we wish to report studies using  $\text{NO}_2^-$  ions, i.e., asymmetric tops. We shall see that the rotation-vibration fine structure is quite complex indeed, but with the knowledge gathered from the  $\text{CN}^-$  system we will be able to

interpret the measurements assuming rotational motions around the three principal axes of the  $\text{NO}_2^-$  ion *plus* translational center-of-mass motion of the ion in its cavity. The present paper,<sup>2</sup> therefore, can be regarded as a test for the model developed in the previous paper as well as an extension to the most general case of molecular motion in solids.

### II. THE INFRARED RESULTS

#### A. Spectra

The experimental techniques were the same as those described in I. Most of the crystals used have been

<sup>2</sup> Part of this work has been briefly presented previously. See V. Narayanamurti, *Bull. Am. Phys. Soc.* **9**, 271 (1964).

\* Present address: Department of Physics, Indian Institute of Technology, Bombay, India.

† Present address: Department of Physics, University of Illinois, Urbana, Illinois.

<sup>1</sup> W. D. Seward and V. Narayanamurti, preceding paper, *Phys. Rev.* **148**, 463 (1966). Hereafter referred to as I.